Climate variability and potential future climate change in southern Amazonia: sensitivity of the hydrological cycle to land use changes

Dissertation

with the aim of achieving a doctoral degree
at the Faculty of Mathematics, Informatics and Natural Sciences
Department of Earth Sciences, University of Hamburg

submitted by

Markus Kilian

in

Hamburg

2017

Day of oral defense: 06.12.2017

The following evaluators recommend the admission of the dissertation:
Prof. Dr. Valerio Lucarini
Prof. Dr. Jürger Böhner

Für Goki und Goko
Meine Großeltern

Abstract

Land use and land cover changes can be important drivers on the local and regional weather and climate system and a source of different feedback mechanisms. Since long, land use and land cover changes are taking place in Brazil. Mainly, deforestation, the clearance of the tropical rain forest was the larges part of the land use change. Over the last decades, however, international protection programs (e.g. REDD and REDD+; Reduction Emission from Deforestation and Degradation), archived the reduction of the tropical rain forest clearing in the biome Amazonia, a reduction of emissions from the deforestation and a reduction of degradation of the vegetation. So, the region of the land use change moved to the south, where environmental protection programs are not as strict as in Amazonia. In this work, the impact of the land use changes on the regional weather and climate system is investigated in the biomes of Cerrado, Pantanal, Mata Atlantica and Pampas. The land use simulated by the LandSHIFT model were implemented in the Weather and Research Forecast model WRF, a regional climate model. The GCM ECHAM5/MPI-OM is used to provide an external greenhouse gas forcing.

To investigate the impacts of the land use change, the 2 m temperature, total precipitation, evaporation and the hydrological cycle ($P - E$) are investigate in the WRF model results on a 60 km and 30 km grid. Due to the land use change the albedo, soil moisture, surface heat capacity, surface emissivity and the surface roughness are modified. Compared with the local and country wide impacts of the greenhouse gas forcing implemented by the ECHAM5 A1B scenario, the local changes due to the land use changes are small. A reason for this small impact is the spatial distribution of the land use change in a dynamical system with a high internal variability. Nevertheless, the 2 m temperature decreases as an effect of the land use change. The strongest cooling occurs in the austral winter in the region of the land use change. The number of cold days, compared to the period 2001–2005, increases significantly in the same region. The total precipitation is also decreasing, however there are no significant impacts on the number of dry days in Brazil. The evaporation increases due to the land use change and interact with the 2 m temperature decrease. However, these changes are small and on the spatial scale no constant signal can be found. The hydrological cycle weakens due to land use changes. Especially in the south of Brazil, where most of the land use change takes place.

In case of all discussed variables the impact of the land use change counteracts the impact of the climate change. However, these changes are much smaller compared

to the impact of the greenhouse gas forcing. Additionally, sensible biomes with a high bio-diversity are exposed by the anthropogenic land use change.

Zusammenfassung

Landnutzungsänderungen können ein wesentlicher Treiber im Wetter- und Klimasystem und Quelle verschiedener Rückkopplungsmechanismen sein. In Brasilien tritt die Landnutzungsänderung schon seit langem auf. Hauptsächlich die Abholzung des tropischen Regenwalds macht den größten Anteil an der Änderung aus. Durch internationale Schutzprogramm (z.B. REDD und REDD+) konnten die Änderungen in den letzten Jahrzehnten hat sich die Änderung und die damit einhergehenden Emissionen eingedämmt werden. Dadurch verschoben sich allerdings die landwirtschaftlichen Bereiche weiter in den Süden und in weniger geschützte Biome wie das Cerrado, das Pantanal, die Mata Atlantica und die Pampas. Die Landnutzungsänderungen aus dem Modell LandSHIFT wurden in das Weather and Research Forecast Modell WRF, ein regionales Klimamodell, implementiert. Als externer Antrieb diente die Ergebnisse des ECHAM5/MPI-OM Modelles der Treibhausgasänderungen.

Um den Einfluss der Landnutzungsänderungen auf das lokale Wetter und Klima zu untersuchen, wurden die folgenden Variablen in den Ergebnissen des WRF Modells in einer räumlichen Auflösung von 60 km bzw. 30 km betrachtet: die 2 m Temperatur, der Niederschlag, die Verdunstung und der hydrologische Kreislauf (Niederschlag minus Verdunstung). Durch die Landnutzungsänderungen verändern sich die Albedo, die Bodenfeuchte, die Wärmekapazität der Oberfläche, die Bodenrauhigkeit und der Emissionsgrad oder Oberfläche. Im Vergleich zu den durch die Treibhausgase induzierten Klimaänderungen sind die von der Landnutzungsänderung indizierten Änderung klein. Ein Grund dafür, ist die räumliche Verteilung der Landnutzungsänderungen und die hohe interne Variabilität des Systems. Durch die Landnutzungsänderung sinkt die 2 m Temperatur. Dabei tritt die stärkste Abkühlung im sudhemisphärischen Winter, in der Region der Landnutzungsänderungen auf. Die Anzahl der kalten Tage, verglichen mit der Periode 2001–2005, steigen in der selben Region signifikant an. Der Niederschlag nimmt ab, wobei es keine signifikante Änderung der Zahl an trockenen Tagen in Brasilien gibt. Die Verdunstung nimmt durch die Änderungen der Landnutzung zu und interagiert mit der abnehmenden 2 m Temperatur. Diese Änderungen sind klein und in der räumlichen Betrachtung ist kein konstantes Signal zu finden. Der hydrologische Kreislauf wird durch die Landnutzungsänderungen abgeschwächt. Die geschieht besonders im Süden, der Region in der die Landnutzungsänderungen stattfinden.

Bei allen hier betrachteten Variablen ist der Trend durch die Landnutzungsänderung

gegenläufig zu dem Trend der durch den Klimawandel generiert wird. Allerdings, sind die Änderungen durch die Landnutzungsänderung vergleichen mit dem Einfluss der Treibhausgase gering. Hinzu kommt, dass durch die Landnutzungsänderung sensible Biome mit einer hohen Bio-Diversität gefährdet sind.

Contents

Chapter 1

Introduction

1.1 Motivation and background

In recent years, the impact of human activities on the climate system and other parts of the earth system has received more and more attention. Especially in the light of the periodic releases of the IPCC reports (Christensen and Hewitson, 2007; Davidson and Metz, 2000; Stocker et al., 2013), the public became increasingly aware of the multiple impacts human activity has on oceans, glaciers, ice sheets, tree cover and whole ecosystems. In the 20th century human impact has reached such a level that today many consider Earth to have arrived in a new age "the anthropocene" (Zalasiewicz et al., 2008, 2015). But despite of all the increased human activity since the industrial revolution, we should not overlook the profound impacts on Earths environment human activity caused since they first appeared on the surface of the earth. The landmark event, which kicked off the anthropocene, is the invention of agriculture and cattle farming in the fertile crescent roughly 10,000 years ago. It can be seen as the Agricultural Revolution. Instead of hunting and gathering plants, they invested most of their time in caring about few animals and plant species. First at a very slowly increased rate the first empires (like the Qin dynasty in Asia or the roman empire in Europe and North Africa) deforested huge areas. This development culminated in the 20th century with a massive increase in intensive industrialized farming reaching in every corner of the world. The increased food production then allowed it already in medieval times to modulate the surface of the earth even further by creating large cities and a dense transportation infrastructure (e.g. highways, airports, channels). Hence, the expansion of human civilization was only possible because of deforestation, fire clearing, settlement, ur-

banization and the creation of farm land.

I therefore want to shed some light on the way land use change has impacted the regional climate in Brazil since here human activity is increasing and has not yet reached a saturation compared to Europe. My aim is clarifying how the local land use change (especially the creation of farm land) impacts the regional climate in contrast to the observed and expected global warming caused by the growing emissions of greenhouse gases.

Land use change is the conversion from a natural vegetation or a natural ecosystem to another vegetation type or ecosystem. Whenever the land use cover is changed, either by natural or anthropogenic processes, there are impacts on the regional weather and climate system. These impacts on the weather and climate system are based on a combination of biogeophysical and biogeochemical effects. Potentially, the impact on the climate or weather can also generate a feedback on to the land use cover further modifying it.

There are many famous examples of feedback mechanisms. One of them is the Taiga-Tundra feedback. If a forest expands rapidly in a cold climate (mainly in higher latitudes), it replaces a high albedo land use cover (mainly snow-covered areas) with low albedo dark green forests. This increases the heat fluxes at the surface leading to an even more rapid expansion of the forest. If this also leads to a melting of the permafrost soil the consequential release of methane further intensifies this positive feedback loop. But of course there are also other examples of a positive feedback like the Charney feedback loop. Charney et al. (1975) investigate a biogeophysical feedback mechanism in the drought of the Sahara. Here, the albedo increases from a decrease in plant cover. This change in the albedo causes a decrease in the local precipitation. In the end, the decrease of precipitation can lead to a decrease in the plant cover and so reinforce the albedo decrease. This positive feedback can strengthen itself and can cause drought events or even desertification.

Another example of land use change is urbanization. On a very local scale the albedo, soil moisture, thermal inertia of the surface and the heat capacity are drastically changed. This leads to an urban heat island (Oke, 1973; Kim, 1992). With buildings and tarmac streets the albedo decreases and absorbs much more solar radiation. Due to the much higher heat capacity, the urban area tends to stay warm. Especially at night the urban heat island raises the temperature. A secondary effect of the urban heat island are a modification in local wind patterns since local convection is inhibited. Other secondary effects are a higher air pollution. More

condensation nuclei can change the pattern of the precipitation in and near the urban area. Eventually, such changes modify local convection patterns which can influence precipitation and temperatures substantially. Additionally, due to intense air pollution more particles for condensation are available which strengthen the positive trend in precipitation.

The Earth surface influence and interacts with the atmosphere, and so the climate through biogeophysical and biogeochemical effects. Prominent examples of a biogeophysical interaction are ice-albeo feedback mechanism, the Charney feedback in the Sahara and the Taiga-Tundra feedback. Changes in the vegetation leads to changes in the leaf area index, the albedo, evapo-transpiration and the root depth (Mahmood et al., 2010; Pielke et al., 2011). Biogeochemical examples are the exchange of carbon dioxide (CO_2) of dust and organic compounds.

Focusing on South America, land use change occur mostly in the Amazon rain forest, where large parts of the tropical rain forest are deforested and destroyed by fire clearing. In 1990 in Brazil 5,467,059 km^2 are covered with forest where only 25 years later in 2015 4,935,380 km^2 are covered with forest, so within these 25 years the area of the Brazilian forest decreased by 9.73%. Most of this area where converted into agricultural areas. An increase of the population explains the need of agricultural areas. Since of 1960, where Brazil had 72,207,554 inhabitants population grown by factor 28 until 2016 when 207,652,865 people lived in Brazil. Agricultural areas and crop production is also need in the economic sector. Brazil is the fourth largest food exporter in the world.

This work is based in the CarBioCial projected (Carbon sequestration, biodiversity and social structures in Southern Amazonia). In the Amazon rain forest and the Cerrado biome, forest clearing takes place to gain areas for cattle farming and crop cultivation. After a few years of forest clearing the soil is depleted and degenerated, which means that it only contains a low level of nitrates, phosphates and is very poor in organic material and furthermore has a high acidity. To handle these problems the CarBioCial project was set-up to create a scientific based decision supporting system with the aim of a sustainable land management under scientific consultations. In the direct contact with stakeholders and local farmers practical recommendations are attended, e.g. avoiding huge mono-cultural areas and having instead a mixed landscape with bushes and trees. This would help to fix and bind carbon in the soil and enhance and enrich the soils in Brazil. Binding greenhouse gases will also have a positive impact on the climate system. This project can even be a blue print for similar regions all over the world.

This work is focused on the land use and land cover changes in Brazil with the impact on the regional weather and climate system. In order to investigate these impacts, a regional climate model coupled to a socio-economic land use and land cover model is used on a high spatial and temporal resolution scale.

Previous studies, for instance Lejeune et al. (2014), show a random distributed land use change or even a total deforestation. Most of the studies have a strong focus on the amazon rain forest deforestation (e.g. Pires and Costa (2013); Swann et al. (2015); Bush et al. (2016); Nobre et al. (2016); Guimberteau et al. (2017); Khanna et al. (2017); Zemp et al. (2017)) or even only the districts of Amazonia or Mato Grosso (Pongratz et al., 2006). Other studies, for instance Fersch (2011), investigate the impact of the land use and land cover change in the past. In 2013 a large part of publications (54 out of 73 publications) of land use and land cover change (LUCC) climate feedback related papers have a focus on Amazonia where only a small part (the remaining 19 publications) addresses non-Amazonia regions (Marris, 2005; Costa and Pires, 2010; Salazar, 2016). Results from the socio-economic land use and land cover model show that in the future the regions with the highest land use and land cover change will be in the Cerrado biome, a region in the central of Brazil south of the Amazon rain forest, and large areas in Rio Grande do Sul, the southernmost district of Brazil. This prediction is implemented in the socio-economic land use and land cover model used in this work. Malhado et al. (2010) argue that, by protecting the Cerrado, the Amazon rain forest will be protected as well due to regional climate effects on both ecosystems.

Since the Amazon rain forest is more monitored and protected over time (see forest monitoring program Brazil ENREDD+ (Reducing Emissions from Deforestation and Degradation ; ENREDD+ (2016)) and GEO4 (UNEP, 2007)) future LUCC and increased need of crop lands will strengthen the trend of shifting to different regions. Over the last decades of the twentieth century the deforestation of the Amazon rain forest slowed down but, nevertheless, increased in the neighboring Cerrado, where the regulations are less strict (Spangler et al., 2017).

These short spatial scale differences in land use change can have an impact on the local scale convection as well as the local hydrological cycle (e.g. Rieck et al. (2014); Rieck (2015)). Especially with a random distributed land use and land cover change these effects can overestimate local effects. I want to show the effects on a realistic scenario applying the socio-economic driven land use scenario in this work.

1.2 Weather and climate system of South America and Brazil

The weather and climate system of South America is affected by different climate drivers. Through the large extension of the research area (see the domain in Figure 1.1) and the position near the equator it is necessary to take the global circulation into account: The Headly cell, the Walker circulation, the El-Niño-Southern-Oscillation (ENSO) (Trenberth, 1997; Dai and Wigley, 2000) as well as the Maden-Julian-Oscillation (MJO) (Madden and Julian, 1971), the Inter tropical convergence zone (ITCZ), the South Atlantic convergence zone (SACZ) (Liebmann et al., 1999; Barros et al., 2000; Robertson and Mechoso, 2000) and the South American Monsoon System (SAMS) (Carvalho et al., 2011; Liebmann and Mechoso, 2011).

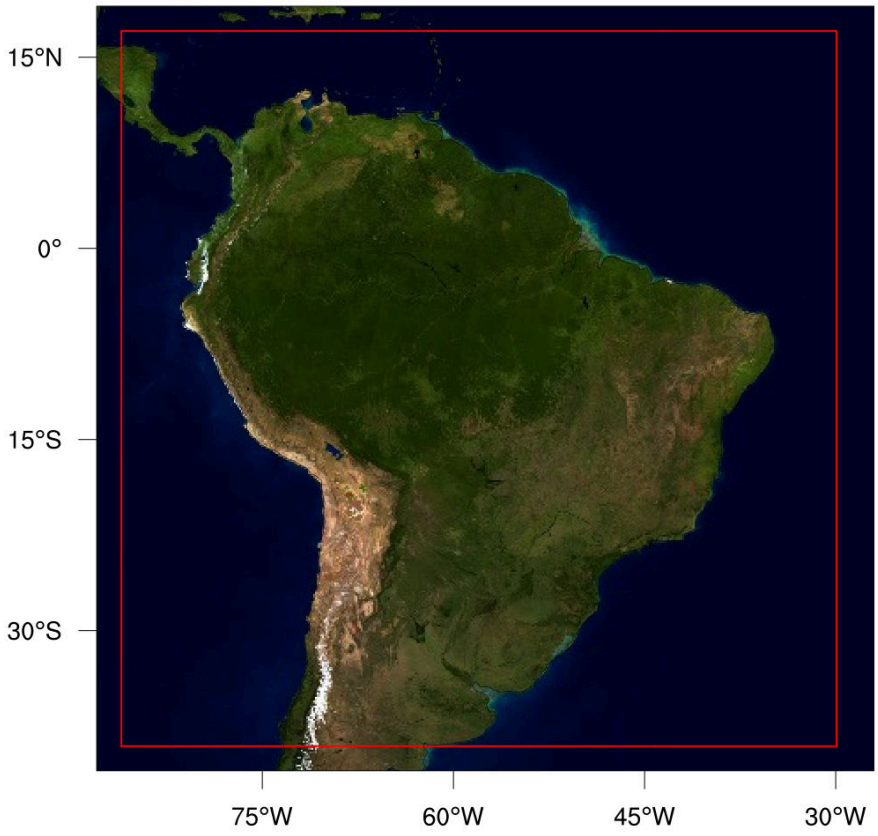

Figure 1.1: Domain of South America where the region of interest is marked (red box). The image is based on the Earth Map provided by the NCAR (source: https://www.ncl.ucar.edu/Applications/Scripts/EarthMap_2500x1250.jpg).

Globally, air masses near the equator are heated most due to a direct and stronger

insulation.

These warm air masses in these regions rise and diverge at the tropopause with, warm and humid air masses convergence near surface. The area is known as the Inter Tropical Convergence Zone (ITCZ), which is part of the Hadley circulation. The ITCZ with its strong convergence and updraft of warm and humid air masses creates a huge amount of convective available potential energy (CAPE), thunderstorms and strong large-scale precipitations. The position of the ITCZ varies on annual time scales due to solar irradiation changes caused by the Earth's axial tilt (obliquity). This convergence zone with its raining belt move over the year from north (in boreal winter) to south (in boreal summer) and backwards. In addition to this meridional movement a zonal circulation, the Walker circulation, also affects the climate and hydrology in South America. The strongest cell of the Walker circulation has an upward branch near Indonesia and a downward branch over the Pacific Ocean near South America. Changes in the strength of this circulation, which is coupled to the oceanic circulation as well, are called El-Niño-Southern-Oscillation. The impact of the ENSO on the South American climate system is strong and affects the temperature and precipitation (Grimm and Natori, 2006). Recent investigations have shown an increase in surface temperature, atmospheric stability, surface shortwave down-welling radiation and a decrease in cloudiness, seasonal mean convection and moisture transport take place (Dai, 2006; Warren et al., 2007; Arias et al., 2011)

Future climate projections show a temperature increase till the end of the 21th century (Christensen and Hewitson, 2007). In the IPCC Special Report Emissions Scenarios A1B (SRES; Davidson and Metz (2000)) scenario the temperature will increase by more than 2.5 K for the region of Brazil (Figure 1.2), where in some regions the temperature will increase up to 6-8 K until 2100 compared to the present state (Marengo et al., 2010). In contrast to temperature changes, modeled precipitation changes are not consistent. Most of the model simulations indicates a significant increase of the annual precipitation until the end of the 21th century (e.g. GISS-EH, GISS-ER, IPSL-CM4), whereas other models indicate a significant decrease (e.g. UKMO-HadCM3, GFDL-CM2.1) or even no significant changes (e.g. ECHAM5/MPI-OM, INM-CM3.0, MRI-CGCM2.3.2; Li and Zeng (2002)). However, for the whole domain significant changes in the precipitation extremes as well as in the dry spells are also projected, where especially in the southeastern- and southern South America an increased intensification of extreme precipitation events until 2100 will take place (Marengo et al., 2009). Additionally, Vera et al. (2006) have shown an increase of summer precipitation but a decrease of winter

precipitation in southeast South America.

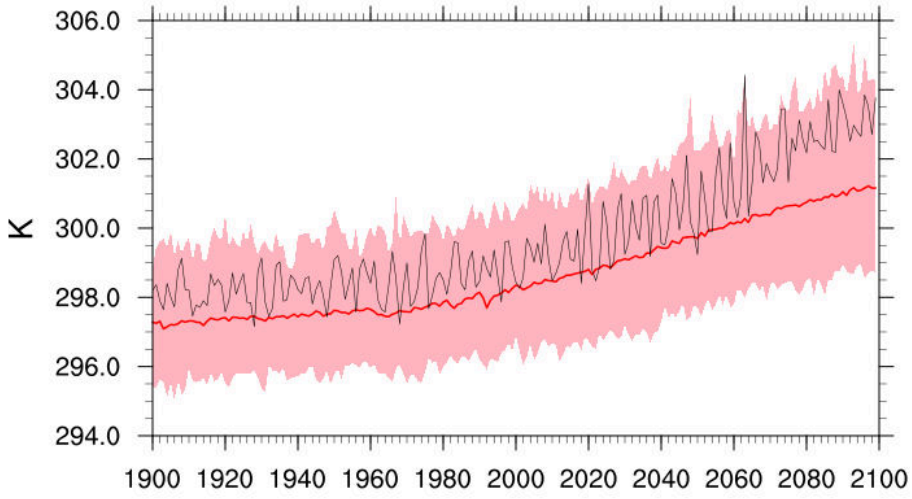

Figure 1.2: Ensemble spread (red shading) of the 2m temperature (in Kelvin) from the SRES A1B climate models with the ensemble mean (red) and the ECHAM5 A1B model (black).

The hydrological cycle

The hydrological cycle is a cycle of water in all three phases from the surface (and subsurface) to the tropopause. Through evaporation and evapo-transpiration (from vegetation) water-vapor is transported into the atmosphere. The evaporation dependence on the available water, local temperatures and the saturation of water-vapor in the atmosphere. Through changes of the phases of water latent heat can have a feedback on the temperature and the hydrological cycle. The closing branch of the cycle is the condensation of water vapor at the surface and mainly precipitation in rain, graupel, snow or ice. On a global scale the largest part of the evaporation is based on ocean evaporation ($413 * 10^3\,\mathrm{km}^3$) and only a comparatively small amount is based on evapo-transpiration ($73 * 10^3\,\mathrm{km}^3$). In total $486 * 10^3\,\mathrm{km}^3$ of water are evaporated to the atmosphere and the same amount of water is, since it has to be in balance, precipitated, with $113 * 10^3\,\mathrm{km}^3$ land precipitation and $373 * 10^3\,\mathrm{km}^3$ of ocean precipitation Trenberth et al. (2006). In WRF the hydrological cycle is represented by the physical set-up, especially by the microphysics scheme (see Section 2.1).

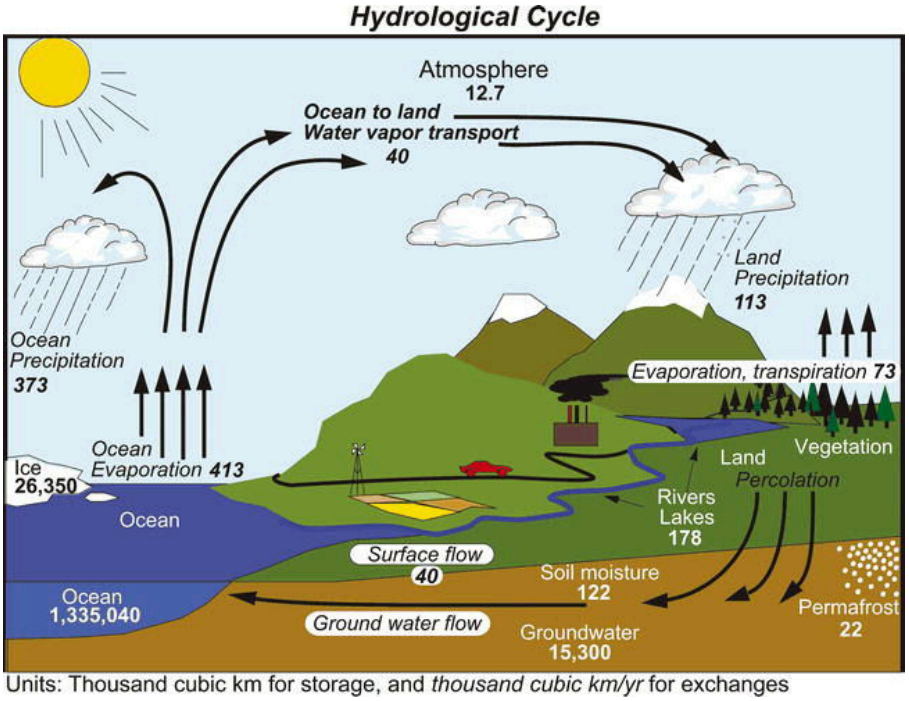

Figure 1.3: Illustration of the hydrological cycle as it moves through the Earth system. Illustration is taken from Trenberth et al. (2006).

1.3 Land use interactions to the weather and climate

Land use and land cover change interact on different ways with the atmosphere and therefore with the weather and climate system. LUCC changes the physical properties of the surface, which are described in the WRF model as changes in albedo (α), roughness length (z_0), soil moisture ($SLMO$), surface emissivity ($SFEM$), surface thermal inertia ($THERIN$) and soil heat capacity ($SFHC$). However, the vegetation is not simulated by WRF the leaf area index (LAI) and the evapo-transpiration are changed by the different land use initializations. These variables will influence the entire simulated system. In detail, changes in the albedo will directly impact the surface radiation balance (Equation (1.1)). Evaporation and evapo-transpiration changes will have an impact on the latent and sensible heat flux (Equation (1.2)). The evapo-transpiration is linearly scaled to the latent heat flux (Equation (1.3)).

The surface radiation R_n balance, the net energy amount by solar radiation, is defined as the sum of the net shortwave and net long-wave radiation:

$$R_n = S\,(1-\alpha) + L\uparrow - L\downarrow \tag{1.1}$$

where α is the surface albedo, S the incoming shortwave radiation, $L_\uparrow$ the outgoing long-wave radiation and $L\downarrow$ the incoming long-wave radiation at the surface (Peixoto and Oort, 1984).

The net surface energy R_n is defined as the sum of the sensible heat flux (H), the latent heat flux (LH), the ground heat flux (G) and heat flux residuals (R) as (Chen and Dudhia, 2001):

$$R_n = LH + H + G + R \tag{1.2}$$

The evapo-transpiration ET is linearly scaled to the latent heat by

$$ET = 3600\,\frac{LH}{\lambda} \tag{1.3}$$

and is defined as in the Penman-Montaith equation

$$\lambda\,ET = \frac{\Delta(R_n - G) + \rho_a c_p\,(\delta e)\,g_a}{\Delta + \gamma\,(1 + \frac{g_a}{g_s})} \tag{1.4}$$

where λ is the latent heat of vaporization, E the mass water evaporation rate, Δ the rate of change of saturation specific humidity with air temperature, R_n the net radiation, G the ground heat flux, ρ_a the dry air density, c_p the specific heat capacity of air, γ the psychrometric constant , g_a is the conductivity of air and g_s the conductivity of stoma.

Changes due to the evaporation and evapo-transpiration will affect the total water content of the atmosphere with all direct and indirect consequences, for instance changes in the precipitation, cloudiness and cloud convection and the convective available potential energy.

Impacts of deforestation, especially in Amazonia, are widely studied. Lawrence and Vandecar (2014) show that the impact depends on the area and cluster-size of deforestation. Until a critical threshold of land use change precipitation is decreasing by a loss of evapo-transpiration. Khanna et al. (2017) provide evidence, that the change of surface roughness plays an essential role in the local and regional atmospheric circulation, especially in the moisture transport. A decreased surface roughness increases the low level wind speeds which strengthen the moisture

transport. This will directly increase the regional cloudiness and the precipitation frequency. They conclude, that Amazonian deforestation causes a shift from a thermally to a dynamically hydro-climatic regime.

Based on WRF simulations Shi et al. (2014) show for China the effects of land use and land cover changes. They increased the cultivated area by 288,000 km^2 until 2040, which revealed no clear spatial temperature and precipitation trend on a yearly scale. In contrast, they found significant changes on a seasonal scale with larger differing temperature trend among the region.

The effects of the albedo on the occurrence of droughts are studied for the Saharan region by Charney et al. (1975). They explored that due to an increased albedo the moisture convergence and precipitation will decrease. This will strengthen the increase of the albedo and creates a positive feedback mechanism, the so called Charney feedback.

1.4 Present and historical land use change

Brazil is divided in five large biomes with different vegetation and land use types (see Figure 1.4). The most known biome is Amazonia with dense tropical rainforests but also seasonal forest and savannas. In the south of Brazil, Paraguay, Uruguay and Argentina the Pampas is located and a subtropical grass steppe. As a vast tropical savanna, the second largest Brazilian biome is the Cerrado. It includes woody savannas, savannas and savanna wetlands as well as gallery forests. The Cerrado is situated in the districts of Mato Grosso, Goiás, Mato Grosso do Sul, Tocatins, Federal District, São Paulo, Minas Gerais, Piauí and Maranhão. The Pantanal is compared to the other Brazilian biomes small, however it is the world's largest tropical wetland and situated in Mato Grosso do Sul, with parts in Mato Grosso and even Bolivia and Paraguay.

Land use and land cover change took place in Brazil since long and all biomes were and are affected. However, the knowledge of the historical land use conditions is vague and most publications focus on the present time and the future scenarios. Leite et al. (2012) reconstructed the land use change in Brazil from 1940 onwards to 1955. In this period the natural pasture was gradually replaced by planted pastures. Large parts of the Atlantic Forest and the Cerrado where deforested and changed into croplands.

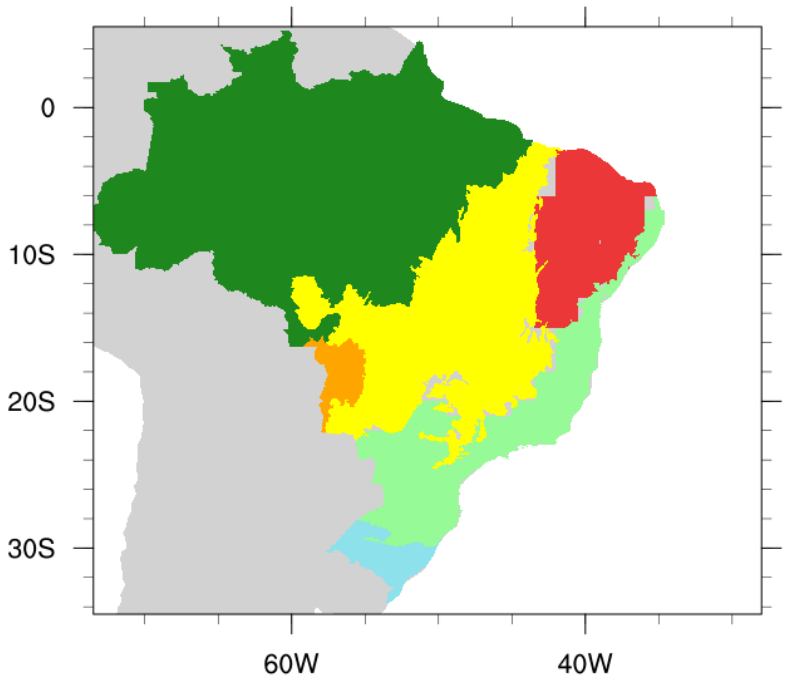

Figure 1.4: Different biomes of Brazil: Amazonia (dark green), Cerrado (yellow), Pantanal (orange), Mata Atlântica (pale green), Caatinga (red) and Pampas (light blue)

Since 1960, croplands expanded from the state of São Paulo to the states of Minas Gerais, Paraná, Santa Cataraina and Rio Grande do Sul. Later the croplands expanded over all areas of Brazil. Until 1980 only 0.04% of the area of Amazonas (the federal district) was used as agricultural lands (Imbach et al., 2015), where in other districts like Mato Grosso the percentage of agricultural lands is partly higher. Since 1980 these effects become stronger over each decade and the strongest changes took place in Mato Grosso, Goiás, Tocatins and Maranhão. Recent studies indicate (e.g.Dias et al. (2016)), that the extensification of the land use change slowed down in the near past time. However agricultural land use intense in the regions already used for croplands.

Outline and structure of the thesis

In Chapter two the general description of the models used in this thesis is presented. It contains the model set-up and the methodology applied to the model results. In Chapter three the outcome of the models are analyzed and the 2 m temperature, the precipitation, the evaporation and the hydrological cycle are analyzed and discussed. With Chapter four the summary and consequences of the results are presented and discussed. At the end of this chapter I discuss in the outlook potential future research.

Chapter 2

Models and methodology

To simulate the impact of land use and land cover changes (LUCC) the output of the dynamic and spatially explicit land-use model LandSHIFT (see Section 2.2) were implemented into the regional weather and climate prediction model WRF. From 2001 to 2040, the weather and climate is predicted over large parts of South America with a spatial resolution of up to 30 km and a temporal resolution of 90 seconds, with an hourly output. With this approach the future climate is simulated in a realistic scenario with respect to LUCC and is compared to a control simulation without LUCC.

2.1 WRF

The Weather Research and Forecasting model (WRF version 3.4.1; Skamarock et al. (2008)) used as a regional climate model (RCM) is a numerical weather prediction (NWP) model as well as an atmospheric simulating system. It is a non-hydrostatic, compressible model and can be used for weather prediction as well as climate predictions. The main task of WRF is the down-scaling of results from a global climate model (GCM) to a higher resolution grid. In general, two branches of the WRF model are provided: The Non-hydrostatic Mesoscale Model (NMM) and the Advanced-Research WRF (WRF-ARW). Differences between these to branches are different dynamic solvers, where the NMM is used for real-time weather prediction and the WRF-ARW is used for regional down-scaling or ideal simulations. For the objective of this thesis I aim for a configuration of WRF that is as realistic as possible. Therefore, the WRF-ARW setup is chosen. Different model physics setups are assessed in order to identify the most realistic setup and validate these results with

ERA-Interim data (Dee et al., 2011) from the ECWMF for a historical simulation. The final setup used in this work is also used by Ruiz et al. (2010) and Fersch (2011) for the same region.

The main modules of WRF (see Table 2.1) are the *radiation scheme*, the *microphysics scheme*, the *planetary boundary layer scheme* and the *cumulus parametrization scheme*.

Table 2.1: List of used physical modules used in WRF

Process schemes	Modules
Short wave radiation	Dudhia
Long wave radiation	RRTM
Planetary boundary layer	YSU
Cloud convection	Kain-Fritsch
Land surface	Unified Noah Land Surface Model
Surface layer	MM5
Microphysics	WSM-6

The *radiation scheme* is the main driver of atmospheric dynamics with interaction between the radiation and the surface as well as the atmosphere. Radiation causes heating at the ground and the atmosphere. The short-wave radiation is parametrized by the Dudhia radiation scheme (Dudhia, 1989) where the long-wave radiation is parametrized by the *Rapid Radiation Transfer Model* (RRTM); (Mlawer et al., 1997).

The calculation of small-scale water fluxes in all three phases (liquid, ice and vapor) with all depending variables by the *WRF Single Moment 6 module* (WSM-6) *microphysics scheme* (Hong and Lim, 2006) for instance grid scale precipitation, clouds and water vapor fluxes is provided. The *planetary boundary layer* (PBL) is the lowest level of the atmosphere where most of the important sub-gridscale fluxes take place. Here the *Yonsei University* (YSU) planetary boundary layer scheme for a well-mixed layer is used.

For the representation of clouds in the model, the *Cumulus parametrization scheme*, the Kain-Fritsch (KF) convection scheme with shallow (non-precipitation) convective clouds are used (Kain, 2004).

Regional initialization and model setup

Two simulations are setup up and run with WRF. In both, the land use and land cover were initialized using the LandSHIFT (Schaldach et al. (2013); Section 2.2) model for Brazil and MODIS data for the remaining domain. In the control simulation, the land use and land cover was fixed to the initial conditions from 2001, where in the land use scenario the land use was changed every 5 years based on LandSHIFT the model output. Starting from 2006 every run (e.g. 2006-2010 or 2011-2015) was simulated with one year of spin-up.

On a geographical scale the outer boundaries of the model domain are 39.06° S to 17.06° N and 86.06° W to 29.93° W with a horizontal grid resolution of 60 km × 60 km. The inner domain with a grid resolution of 30 km × 30 km has a slightly smaller size, to avoid boundary effects, with the boundaries 36.49° S to 14.49° N and 83.49° W to 32.50° W; see Figure 2.1 for the boundaries of the outer and inner domain. In the vertical direction the model simulations are set up with 45 levels and 4 soil levels.

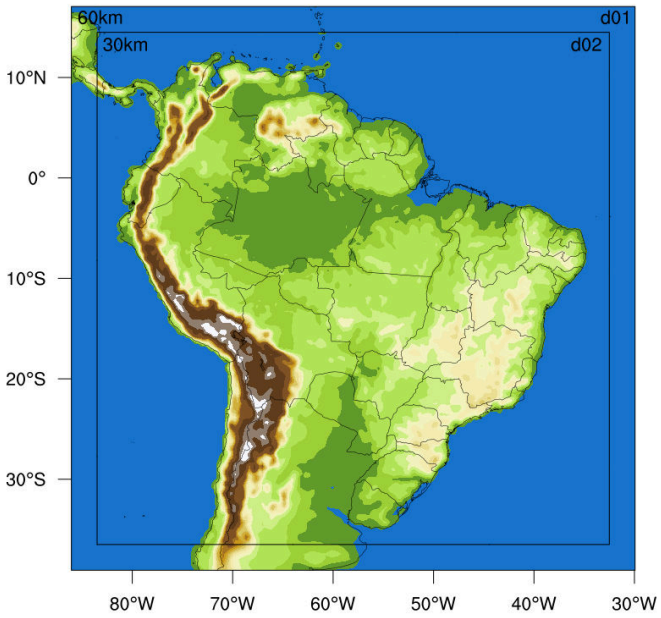

Figure 2.1: The inner (d02) and outer (d01) domain of the WRF simulations.

The external climate driver is provided by the ECHAM5 A1B scenario (Roeckner et al., 2003; Vera et al., 2006; Stocker et al., 2013) to use a realistic climate trend in both domains. It is used as an outer boundary without nudging to keep the internal model physics work proper. The update time of the external driver is set

to six hours where the internal time-step to solve small-scale fluxes and convergences is set to 90 seconds. On each hour of simulation time an output file is generated. The experimental setup is listed in Table 2.2

Table 2.2: Setup of the experiments.

Test	Period	Underlying surface data	Climate forcing data	Spatial resolution
Control run	2001-2040	Land cover of 2001 to 2005	ECHAM5 A1B forcing between 2001 and 2040	60km, 30km
Land use experiment	2001-2040	Land cover of 2001 to 2040, updated every 5 years	ECHAM5 A1B forcing between 2001 and 2040	60km, 30km

2.2 LandSHIFT

The land use and land cover scenario used in the modeling framework was developed for Brazil by the *Land Simulation to Harmonize and Integrate Freshwater Availability and the Terrestrial Environment* (LandSHIFT) model. The aim of the LandSHIFT model is simulating and analyzing spatially explicit land use dynamics. The model simulates land-use and land-cover change on a high spatial resolution of 5-arc-min (Schaldach and Koch, 2009) by describing the interplay between anthropogenic and environmental components (Lapola et al., 2010). It is based on socio-economic driven assumptions (Schaldach et al., 2013) for settlement, crop cultivation, grazing and forestry. The model has been applied and evaluated in the region of the Jordan river (Koch et al., 2008), in the Amazon region (Lapola et al., 2010) and Brazil (Lapola et al., 2009).

The United Nations Environment Programme's (UNEP) Global Environment Outlook 4 (GEO4) (UNEP, 2007) report under the 'Markets first' scenario is used to generate socio-economic projections. The assumptions used in the 'Markets first' scenario is the faith in the market to improve not only the markets, but also the social system and the environment. Private sectors will increase and the role of local governments will decrease. Free trade and a commoditization of the environment will take place under these assumptions. The key question of this scenario is: 'How

risky is it to put markets first?' (UNEP, 2007). However, the environmental protection will progress slowly and most species will decrease with large losses in South America. For agriculture, due to climate change and a growth of infrastructure, the reduction of the terrestrial biodiversity of the past will continue in this future scenario. In comparison to all other GEO4 scenarios (Policy First, Security First and Sustainability First) the global CO_2 concentration in 'Markets first' will be the highest and hit the 550 ppmv in 2050. Due to an intensification of the energy sector the region with the highest CO_2 change will be Latin America and the Caribbean.

Brazil is on of the four countries – Brazil, Russia, India and China, the so called BRIC states – heading the emerging markets. With a population grow from 72,207,554 (1960) to 207,652,865 (in 2014) the need for food production increased dramatical. Since 1961 the agricultural land increased constantly with, whereas in 1961 18.01% of Brazil are covered by agricultural land and 33.81% in 2014. The need in food and additionally for the export is huge and so the crop production index increased from 23.31 in 1961 to 143.48 in 2014 (where $2004 - 2006 = 100$).

These trend will continue Land use and land cover change into agricultural areas (croplands) will take place, however, this trend will be partly compensated due to technical developments.

The land use and land cover are classified into 17 different categories regarding the definition of the International Geosphere-Biosphere Programme (IGBP) (Strahler et al., 1999; Friedl et al., 2002) (see Table 2.3).

The dominating land use type over the South American domain is the evergreen broadleaf forest with 43.5% (54.9% in the total domain) followed by open shrublands with 8.2% (3.67%) and grasslands with 7.6% (3.4%). Within the time period from 2001 to 2040 the land use and land cover changes in the LandSHIFT scenario by transforming parts of the evergreen broadleaf forest, the savannas and the grasslands into cropslands due to an intensification of agricultural land use and a higher pressure on the ecosystem due population growth. In the districts of Mato Grosso, Mato Grosso do Sul, Goiás, Minas Gerais, São Paulo, Rio de Janeiro and Espírito Santo and Paraná savannas will be transformed into croplands. In these regions part of the biomes Cerrado and Pantanal are situated. Additionally, in the district of Rio Grade do Sul grasslands will be transformed into croplands. These grasslands are part of the Pampas biome (Figure 2.2).

With respect to the entire domain (see Figure 2.1), 10.56% of the savannas, and 6.2% of the grasslands will be transformed into croplands. The increase in the area

Table 2.3: List of used land use categories.

Number	Land use type	Fractional area [%]	Area [km^2]
1	Evergreen Needleleaf Forests	0.0726	7,200
2	Evergreen Broadleaf Forests	19.4558	1,967,400
3	Deciduous Needleleaf Forests	0	0
4	Deciduous Broadleaf Forests	1.1882	119,700
5	Mixed Forests	0.0272	2,700
6	Closed Shrublands	0.1723	17,100
7	Open Shrublands	3.6735	370,800
8	Woody Savannas	0.9887	65,700
9	Savannas	9.7868	989,100
10	Grasslands	3.3923	342,900
11	Permanent Wetlands	0.0544	5,400
12	Cropslands	4.8798	493,200
13	Urban and Built-up	0.0272	2,700
14	Croplands / Natural Vegetation Mosaics	0.0272	2,700
15	Snow and Ice	0	0
16	Barren	1.3424	135,000
17	Water Bodies	54.9116	5,552,100

of croplands is 25.84% over the entire domain (see Table 2.4).

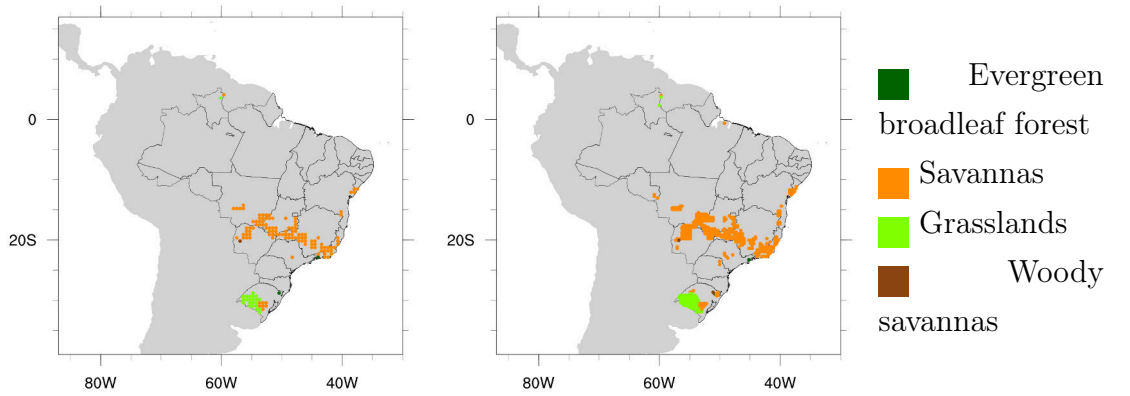

Figure 2.2: Location of the land use change. The color indicates the original land use categories where the evergreen broadleaf forest is dark green, Savannas orange, Grasslands green and woody savannas brown.

Table 2.4: Table of land use changes.

Vegetation Type	Start [km^2]	End [km^2]	change [km^2]
Evergreen Broadleaf Forest	1967400 (19.4558%)	1965600 (19.4376%)	-1800 (-0.093%)
Savannas	989100 (9.7868%)	885600 (8.7528%)	-103500 (-10.566%)
Grasslands	342900 (3.3923%)	321300 (3.1837%)	-21600 (-6.150%)
Croplands	493200 (4.8798%)	620100 (6.1406%)	126900 (+25.84%)

Table 2.5: Table of physical changes.

	Savannas	Grasslands	Evergreen broadleaf forest
albedo	20→18	19→18	12→18
surface moisture summer	0.15→0.30	0.15→0.30	0.50→0.30
surface moisture winter	0.15→0.60	0.30→0.60	0.50→0.60
surface emissivity	0.92→0.935	0.92→0.935	0.95→0.935
surface roughness	15→7.5	7.5→7.5	50→7.5

Chapter 3

Results

Two experiments are driven with WRF. The control run CTL and the land use changed run LUC. The CTL experiment is exposed to only external forcing, the climate change in the ECHAM5 model, whereas the LUC experiment has the land use change as an internal forcing in addition. The impact of the two forcing is investigated on the 2 m temperature, the total precipitation and the evaporation. In addition, the difference between the precipitation and the evaporation ($P - E$) and the ratio of the convective precipitation ($\frac{P_{conv}}{P_{total}}$) are taken into account. On each variable the impact of the climate change and the land use change are separately examined. In the following, the regional average is defined as $\{X\} = \int_{lat1}^{lat2}\int_{lon1}^{lon2} X\,dx\,dy$, whereas the time average is defined as $\overline{X} = \int_{time1}^{time2} X\,dt$. To investigate the impact of climate change, spatial difference plots are created with a reference period from 2001 to 2005. All spatial plots are averaged over five-year time-slices (e.g. 2006-2010 or 2011-2015) in order to be consistent with the simulations, in which the land use is constant in each of the five-year slices. In addition, time series averaged over different regions are presented. To study the impact of the land use change, the absolute values and the difference between both experiments (LUC minus CTL) are investigated on a temporal and spatial scale. The regions used for the area average are Brazil and the land use region (only the regions affected by the land use change). Area average are also performed for the districts of Para, Mato Grosso, Mato Grosso do Sul, Goiás, Minas Gerais, São Paulo, Paraná, Santa Catarina and Rio Grande do Sul.

Seasonal impacts of both forcing are analyzed by calculating the annual cycle of each region per five-year slice. For the winter (JJA) and summer season (DJF) temporal averaged spatial plots are generated.

To test the significance of the difference between both experiments and, in the end, the impact of the land use change on the regional climate a Chi-square test is used to test for statistical independence. The Chi-Square test is defined as follows:

$$\chi^2 = \sum_{i=1}^{i=R} \sum_{j=1}^{j=C} \frac{(n_{ij} - n^*_{ij})^2}{n^*_{ij}}$$

,

where $n^*_{ij} = \frac{n_{i.} * n_{.j}}{n}$ with $n = R * C$, $n_{i.} = \sum_{j=1}^{R} = n_{ij}$ and $n_{.j} = \sum_{i=1}^{C} = n_{ij}$. R is the number of rows and C the number of columns in the matrix.

The null hypothesis (H_0) states that there is no significant difference between the two experiments (i.e. the land use change has no significant impact on the selected variable), whereas the alternative hypothesis (H_A) says that the selected variable differ significantly between the two experiments.

3.1 Temperature

Overall, the temperature increases from 2001 to 2040. Averaged over Brazil, the 2 meter temperature increases by 1.3 K from 23.8° C to 25.1° C. This temperature increase can be directly linked to the increase in greenhouse gases in the ECHAM5 A1B climate change forcing. To visualize the climate impact on the domain of Brazil, the difference in the five-year average between 2036–2040 and 2001–2005 is calculated for the control simulation CLT: $\overline{T2m_{2036-2040}} - \overline{T2m_{2001-2005}}$ (Figure 3.1). Overall, temperature increases with the strongest heating in the south east (the districts of Minas Gerais, Rio de Janeiro and Esprító Santo) with up to 2.7 K. In the south of Brazil (the district of Rio Grande do Sul), the smallest temperature increase occurs with 0.5 K.

The temporal evolution of regional temperature over Minas Gerais is shown in Figure 3.2b, where the blue line indicates the temperature for the CTL simulation and the red line the time series of the LUC simulation. Comparing this figure with the time series of the regional 2 m temperature of Brazil (see Figure 3.2a) a similar five-year pattern can be observed. This pattern is due to the high variability in the ECHAM5/MPI-OM greenhouse gas forcing arising from the ENSO described in Müller and Roeckner (2008) and the tropical variability (Jungclaus et al., 2006).

To investigate the impact of the land use change over the entire period (2001-2040), the difference of the temperature between to experiments ($\overline{T_{LUC}} - \overline{T_{CTL}}$) is

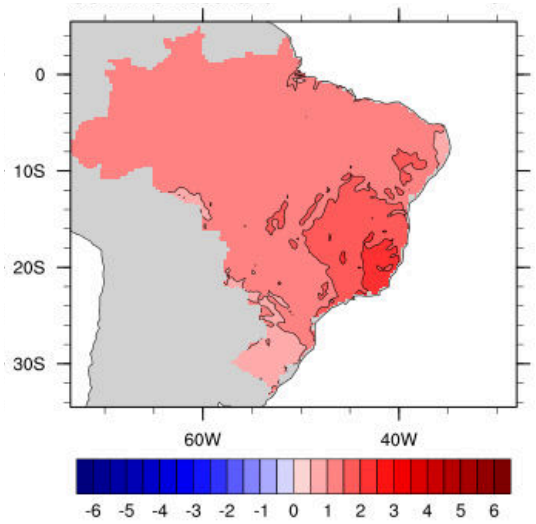

Figure 3.1: Climate change impact in the CTL simulations. 2 m temperature difference between 2036-2040 and 2001-2005.

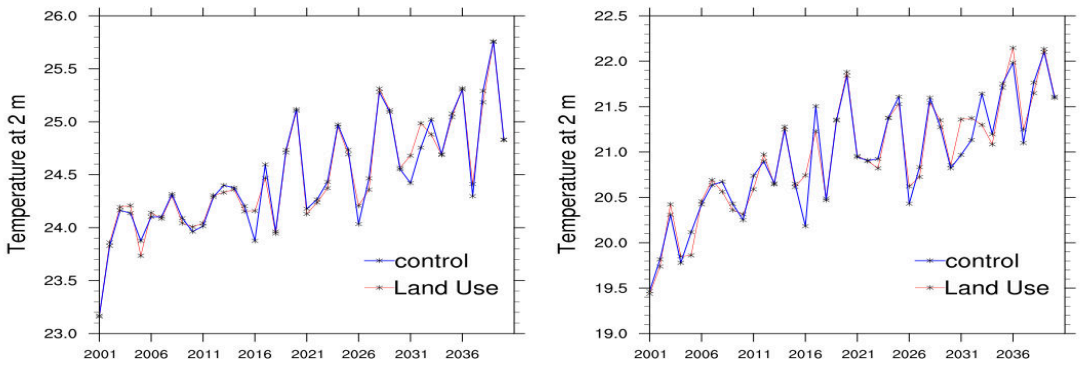

(a) Brazil (b) Minas Gerais

Figure 3.2: Time-series of the 2 m temperature [K] for a) Brazil and b) Minas Gerais

calculated. In Figure 3.3 this difference is shown for the entire period (Figure 3.3a), averaged over the summer (Figure 3.3b) and averaged over winter (Figure 3.3c). The land use change cools Brazil over a large area. However, the temperature change is rather small between -0.3 K and 0.3 K. Average over Brazil the temperature increase and decrease resemble each other. In summer, the amplitude of the positive and negative changes are slightly smaller compared to the total time period. However, average over Brazil the impact of the land use change in summer is rather small (0.01 K). In winter, the cooling due to land use change is the dominant effect with only very few regions showing a warming (up to 0.02 K). The winter cooling is up to -0.47 K and averaged over Brazil -0.05 K.

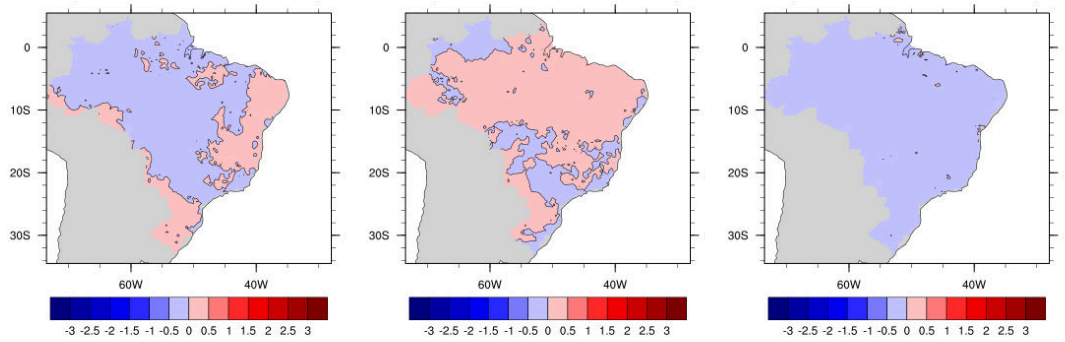

(a) 2001-2040 (b) DJF (c) JJA

Figure 3.3: Difference of the 2 m temperature [K] over the entire time series 2001–2040, summer and winter with respect to the reference period 2001–2005.

To investigate local effects arising from the land use change, a regional average is calculated taken into account only the area and districts affected by the land use change. In Figure 3.4, the time series of these areas is plotted and the overall temperature increase due to increased greenhouse gases is evident. In the upper part of each sub-figure, the time series of both experiments are shown, where the CTL experiment is drawn in blue and the LUC experiment is drawn in red. In the lower part, the differences between the two experiments are shown. For the whole area of the land use change (Figure 3.4a) the temperature decreases in the mean over time. In addition, a high variability can be seen. In contrast to this, in the district of Pará (Figure 3.4b) there is no trend in the temperature but a similar variability, however, on a smaller scale. This fits to the expectation since there is only one grid box in the district affected by the land use change.

The area of the land use change can be divided in two sector, a region in the very south of Brazil in the districts of Rio Grande do Sul and a central region where

the districts from Mato Grosso and Mato Grosso Do Sul to the coast are affected. Representing the central region, the time series of Mato Grosso, Mato Grosso do Sul, Goiás and Minas Gerais show a high variability in the temperature over the whole time period but also a small negative temperature trend. In most of the years the LUC experiment is colder than the CTL experiment.

The temporal variability can be also seen on spatial plots (see Figure 3.5). In each five-year slice, the average of the 2 m temperature of the CTL experiment is plotted on the right hand side. In the middle part of each plot, the average over the same period is shown for the LUC experiment and on the left-hand side the differences between both are drawn. In most figures a cooling due to land use change can be found, however, there are also time periods showing a warming. The cooling is the dominant effect but not only restricted to the regions with land use change. For the period from 2036 to 2040, the 2 m temperature will decrease by -0.45 K ranging between -0.53 K and +0.27 K due to the land use change.

To investigate the impact of the land use change not only five-year time averages or the annual average should be taken into account. It is necessary to focus on the seasonal timescale as well. The annual cycle of each five-year time-slice is calculated. In addition the winter and summer seasons are used to create spatial plots of each five-year time-slide. In Figure 3.6b the green line indicates the five-year average of the 2 m temperature over the area with land use change of the CTL experiment for the time period of 2001 – 2005 and the blue line represents the same average for the period 2036–2040 of the same experiment. The red line represents the 2 m temperature of the LUC experiment averaged over the period 2036–2040. The heating due to increased greenhouse gases (i.e., the difference between the green and the blue line) can be seen. Over whole Brazil, the warming varies by 1.3 K over the months ranging between 0.74 K in December and 1.61 K in April. For the region with land use change, an annual averaged warming of 1.39 K can be observed with the strongest warming in April (1.87 K) and the smallest warming in December (0.49 K). The difference between the blue and the red curve describes the impact of the land use change. The LUC experiment is cooler in every month except December with an averaged cooling of -0.05 K for Brazil and -0.22 K for the land use regions. The strongest cooling occurs in both regions in July with a cooling of -0.27 K for Brazil and -0.66 K for areas affected by the land use change. In December, a warming occurs in both regions with values of 0.22 K for Brazil and 0.59 K for the land use regions.

In the quantile regression, where the 10%, 25%, 75% and 90% percentile are plotted

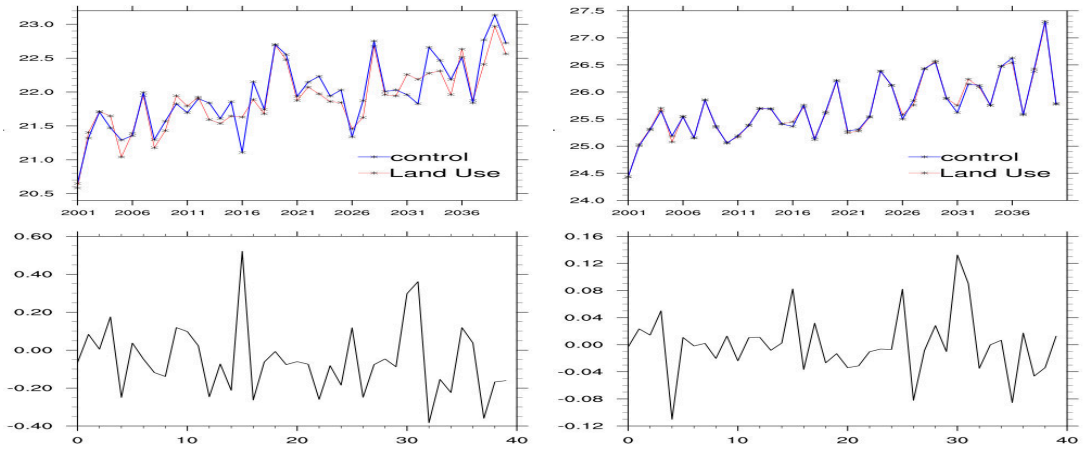

(a) Land use changed region

(b) Para

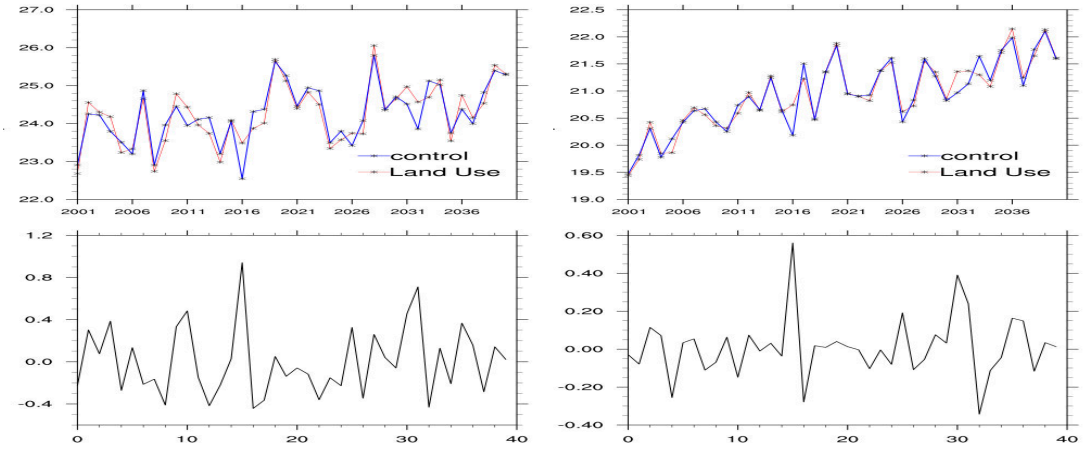

(c) Mato Grosso do Sul

(d) Minas Gerais

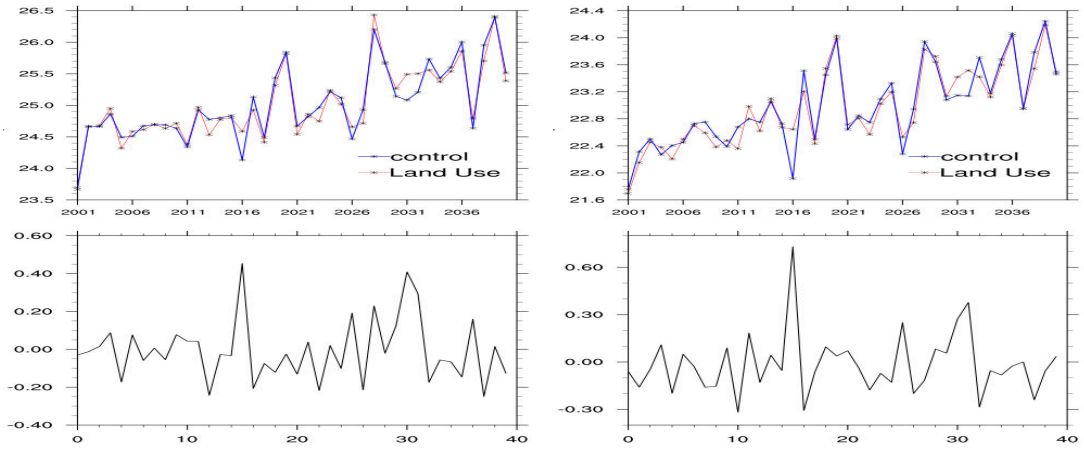

(e) Mato Grosso

(f) Goias

Figure 3.4: Area average of the time series of 2 m temperature [K] over different regions.

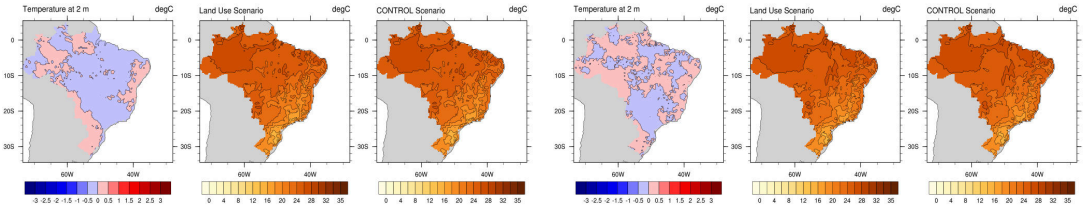

(a) 2001-2005

(b) 2005-2010

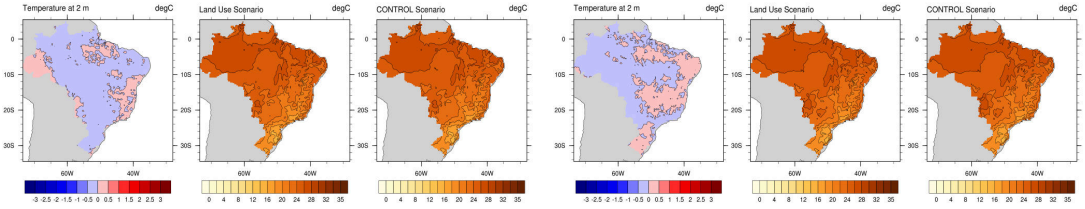

(c) 2011-2015

(d) 2016-2020

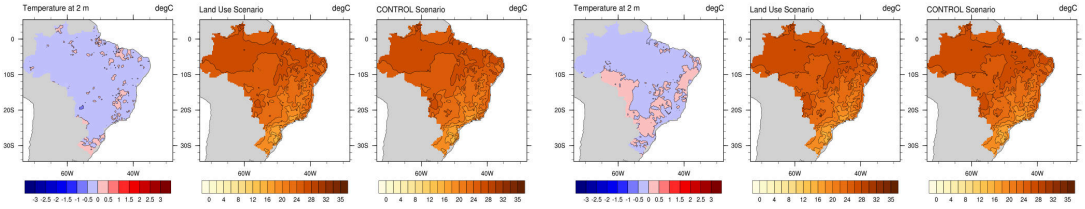

(e) 2021-2025

(f) 2026-2030

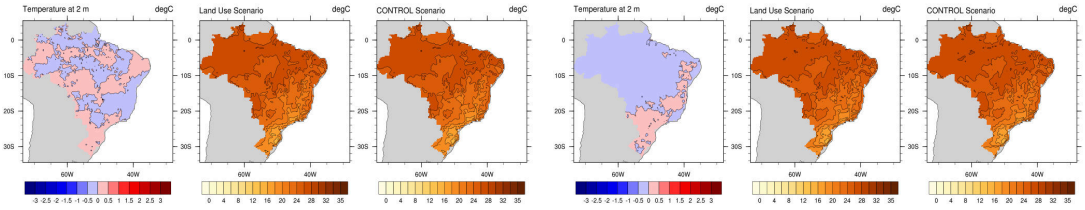

(g) 2031-2035

(h) 2036-2040

Figure 3.5: Contour plot of five-year average of the 2 m temperature [K] in Brazil.

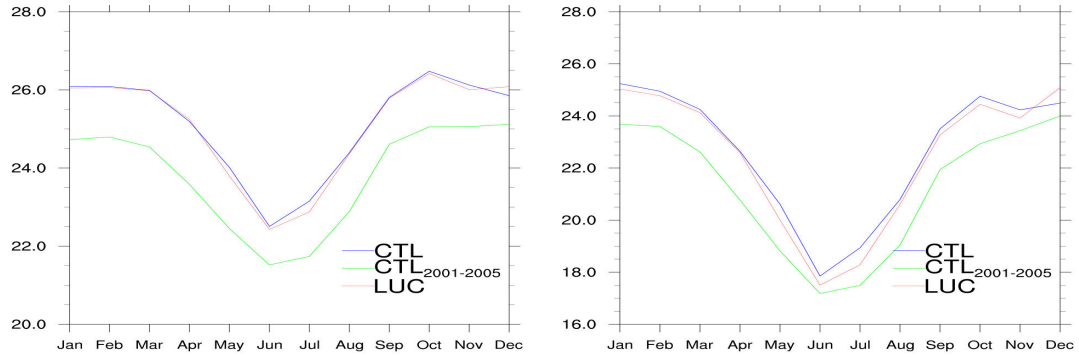

(a) Brazil (b) Land use region

Figure 3.6: Annual cycle of the 2 m temperature [K] for the period 2036-2040 for a) Brazil and b) LUC region.

in gray, the median in blue and the ordinary least square (OLS) regression in red, the negative temperature trend in Brazil and stronger in the region of the land use change can be seen. For Brazil, the slope of the OLS is -0.03, whereas in the land use areas it is -0.176. Since the median and the OLS lines are close to each other the distribution of the monthly temperature anomalies is symmetric.

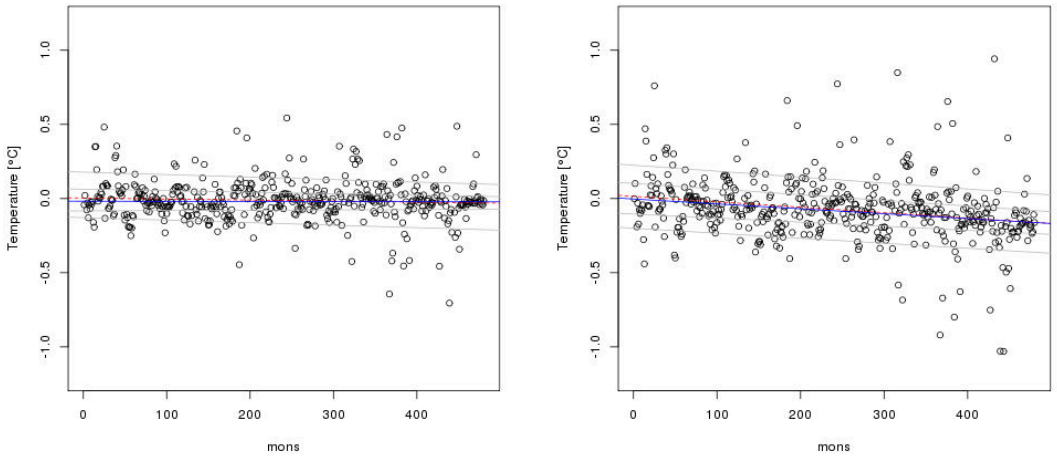

(a) Brazil (b) Land use region

Figure 3.7: Quantile regression of the 2 m temperature for Brazil and the region of land use change.

For the 2 m temperature Chi-square test is performed to test the significance of the results. Assuming that the cooling in the 2 m temperature is due to the impact of the land use change. I counted the number of negative temperature anomalies in the

period 2036–2040 compared to the reference period 2001–2005 in both experiments. To test the alternative hypothesis, $1 - p$ is plotted in Figure 3.8. $1 - p$ shows the probability that the results supports the alternative hypothesis (i.e. the difference in the 2 m temperature are due to the land use change). Regions with the highest significance are shown in blueish colors. Comparing Figure 3.8 with the regions of the land use change (see Figure 2.2), it is clear that besides some regions in the north of Brazil - most statistically significant changes occur in or close to the regions of the land use. Hence, I can conclude that the applied land use change reduces statistically significant the temperature over these regions.

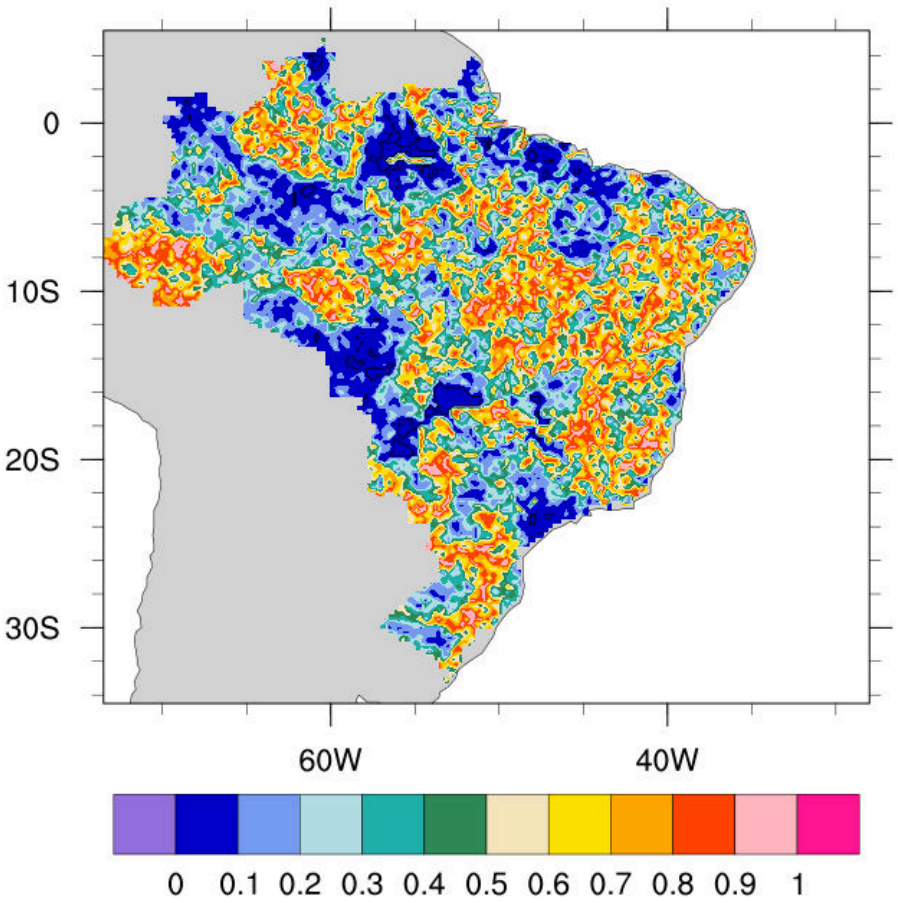

Figure 3.8: p values of the Chi-Square test. Lower values indicates higher significance of a change.

3.2 Precipitation

The total precipitation, in the following only denominated as precipitation, is the sum of the convective precipitation and the advective precipitation. In contrast to the homogeneous temperature signal due to climate change (i.e. the temperature increase all over Brazil), the precipitation change is inhomogeneous. This agrees with the precipitation trend in the climate change forcing and with non-significant precipitation changes in ECHAM5 discussed by Dai (2006). Averaged over Brazil, the trend in precipitation decreases by -0.40 mm/day in the period 2036–2040, with a range between -8.02 mm/day in the north east coastal area and 7.55 mm/day in the south east coastal areas. In Figure 3.9, the change in precipitation due to climate change is shown for Brazil. The difference is defined as $\overline{P_{2036-2040}}$ - $\overline{P_{2001-2005}}$. In large parts of Brazil an increase in precipitation can be seen. However, with respect to the entire time series (Figure 3.10), the last five years (2036–2040) tend to be drier than the previous years. Hence, the negative trend seen in Figure 3.10 in only valid for the period 2036–2040. Some areas in the tropical rain forest and, especially, the coastal area south of Rio de Janeiro show a small increase in precipitation by 2036–2040.

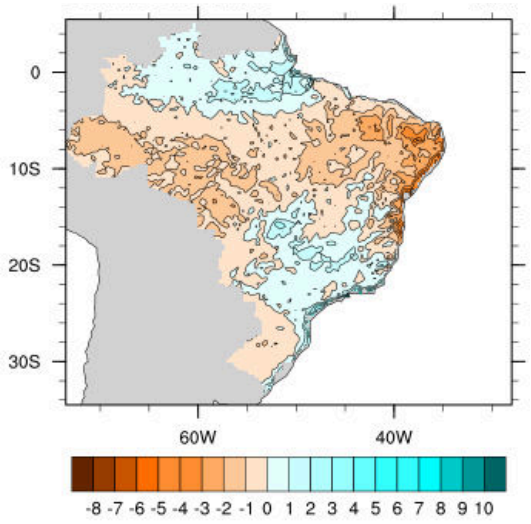

Figure 3.9: Climate change impact of precipitation in the CTL simulations for the period 2036–2040 in mm/day.

Comparing the timeseries of the CTL experiment and the LUC experiment over Brazil only a slight difference can be determined, however the difference becomes larger over time (see Figure 3.10).

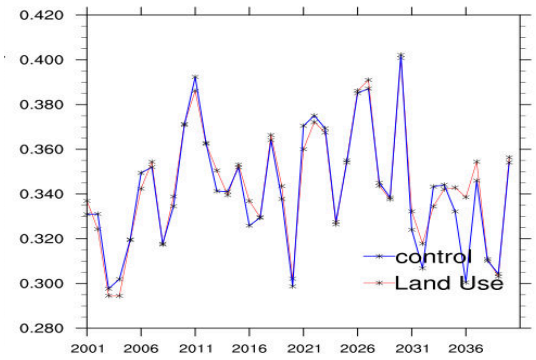

Figure 3.10: Time series of the Brazilian precipitation [mm/day] from 2001 to 2040 for the CTL simulations (blue) and the LUC simulations (red).

Focusing only on the area with applied land use change (same region as in Figure 3.4) a high variability and no clear trends in precipitation be observed in all regions (see Figure 3.12). This high variability is partly related to the variability implied by the ENSO, already discussed for the 2 m temperature (see Section 3.1).

The land use change clearly influences the precipitation (although without clear trend), as the differences between the experiments are larger in Figure 3.12 than in Figure 3.10. Only the district of Para exhibits very similar total precipitation in both experiments, but there only one grid box is affected by the land use change.

The total precipitation averaged over the entire period of 2001–2040 is shown in Figure 3.11a, in Figure 3.11b only December, January and February (summer) months are selected and in Figure 3.11c the winter months June, July and August are selected. Over the whole year the precipitation slightly increases, whereas in winter the precipitation decreases.

Hence, the annual signal is dominated by the change in summer (see Figure 3.11b). The different winter and summer response to the land use change is mostly likely due to the high internal variability, as the decrease largely occurs in areas without land use change. Indeed, the areas with land use change show an increase in precipitation in austral winter.

Analyzing the seasonal differences more in detail, Figure 3.13 shows the annual cycle in precipitation for the period 2036 – 2040. Compared to the reference period (2001 – 2005) the precipitation increases in the CTL experiment throughout the year. The largest increase occurs in the summer months (DJF). The land use change leads to an additional increase in the precipitation over whole Brazil, with the largest increase in austral winter and the smallest increase in austral spring. Focusing on the area of the land use change the precipitation decreases due to

the land use change with strongest decrease in austral summer. This disagrees with Figure 3.11, where I find a general increase in precipitation in austral summer. However, Figure 3.11 shows the mean over the whole time series, whereas Figure 3.13 concentrates only on the last five years. To evaluate this difference, the difference between the two experiments is investigated in each five-year slice (see Figure 3.14). For each five-year period three figures are provided showing the absolute average of the CTL (right) and the LUC experiment (middle) and their difference (left). The high temporal variability is evident, as some time periods show an overall decrease in precipitation (2001–2005, 2006 – 2010 and 2021 – 2025) and some an overall increase. In the last time period the precipitation decreases in large parts of the land use change areas. This explains the decrease in the annual cycle due to land use change seen in Figure 3.13.

To visualize trends in the precipitation for Brazil and the region of the land use change, a quantile regression is performed (see Figure 3.15), as described for the temperature, with 10%, 25%, 50% (blue) 75% and 90% percentiles and the ordinary least square (OLS - red). The OLS regression for both regions (Brazil and land use change region) signifies a negative trend in the precipitation. For the area of the land use change the trend is stronger than for the region of Brazil. Although, the median for the land use region has a negative trend, the slope of the percentiles is similar to both the median and the OLS. Hence, there is no change in the number of extreme precipitation events (5% percentile and 95% percentile).

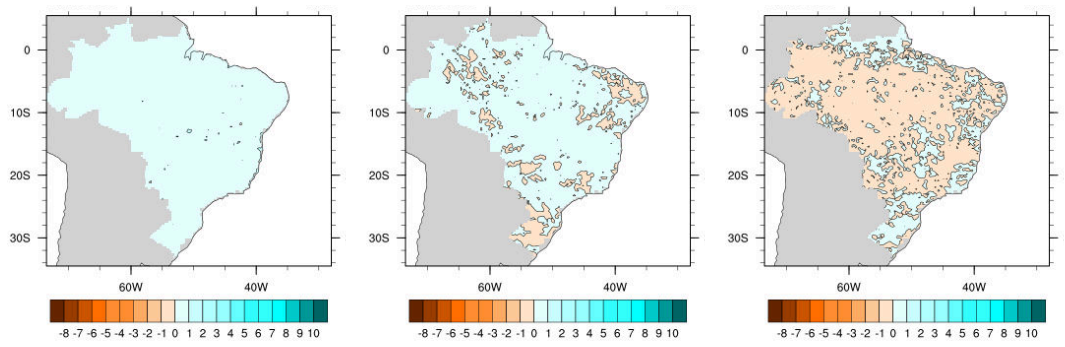

(a) 2001-2040 (b) DJF (c) JJA

Figure 3.11: Difference of the precipitation [mm/day] over the entire time series, summer and winter with respect to the reference period 2001–2005.

To evaluate the statistical significance of the above-mentioned results, a Chi-Square test is applied. The alternative hypothesis is a decrease in precipitation due the land use change. To test this, the number of dry days in the period 2036–2040 compared

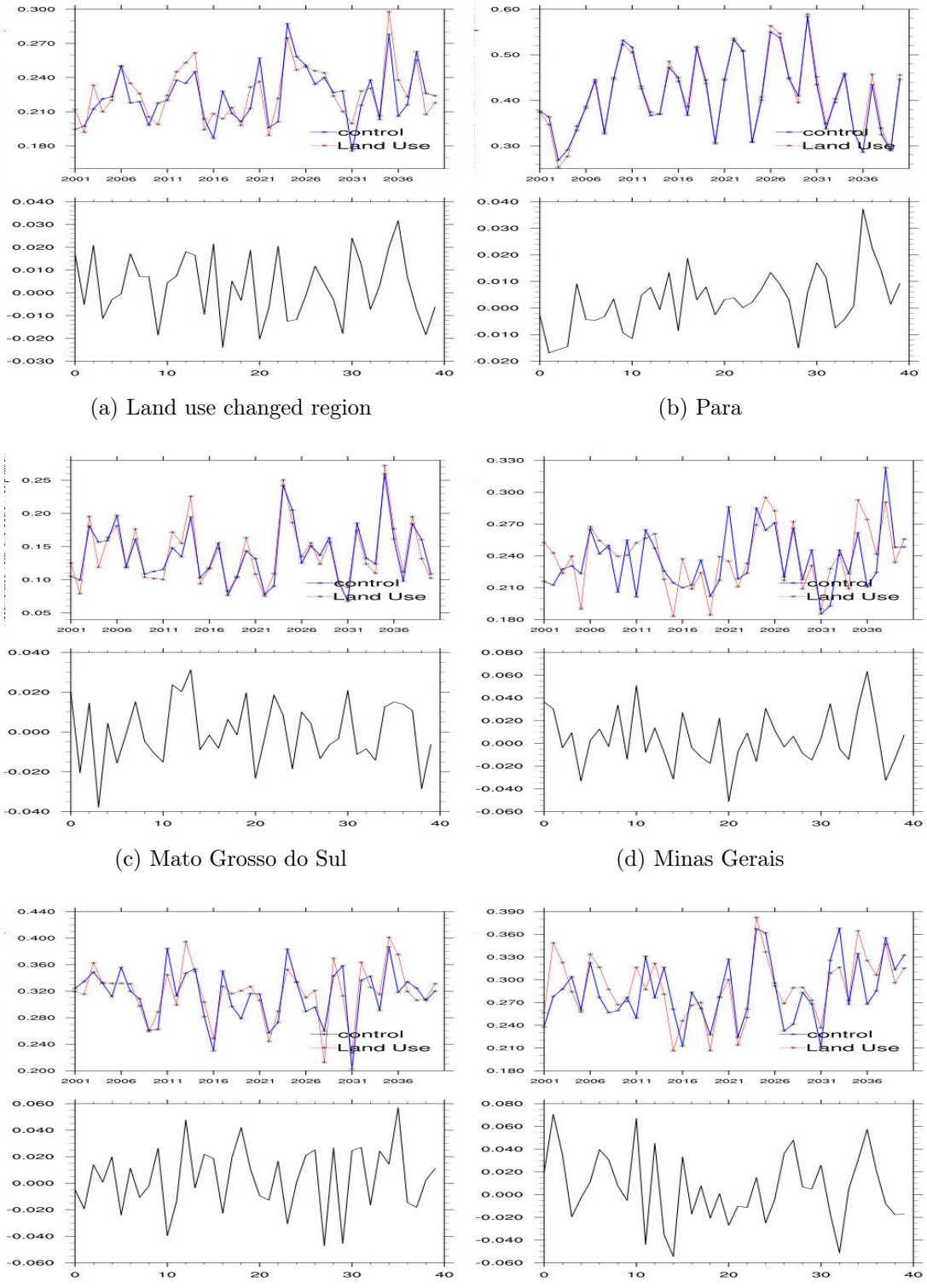

(a) Land use changed region

(b) Para

(c) Mato Grosso do Sul

(d) Minas Gerais

(e) Mato Grosso

(f) Goias

Figure 3.12: Area average of the time series of total precipitation [mm/day] over different regions

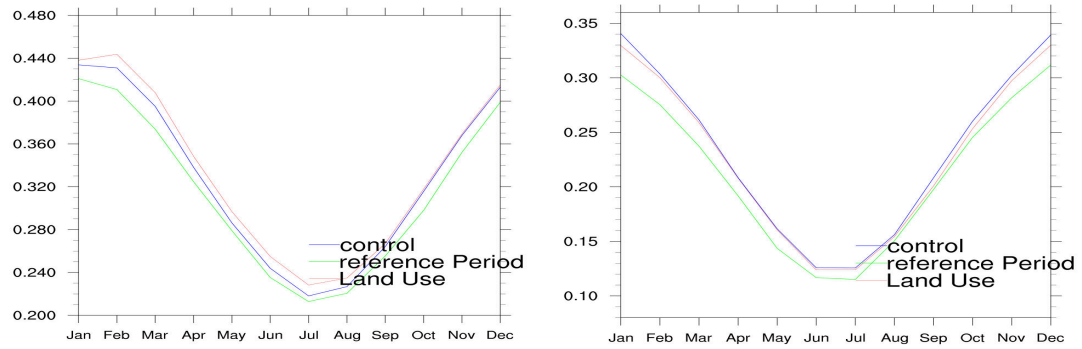

(a) Brazil (b) Land use region

Figure 3.13: Annual cycle of the precipitation [mm/day] for the period 2036-2040 for a) Brazil and b) LUC region.

to the period 2001–2005, are counted. In Figure 3.16 shows the $1 - p$-values of the alternative hypothesis, where small values indicate a high significance. In most parts of Brazil the change in the occurrence of dry days are not significant. However, in central Brazil and in the north-eastern regions few areas have significantly more dry days in the LUC experiment than in the control experiment CTL.

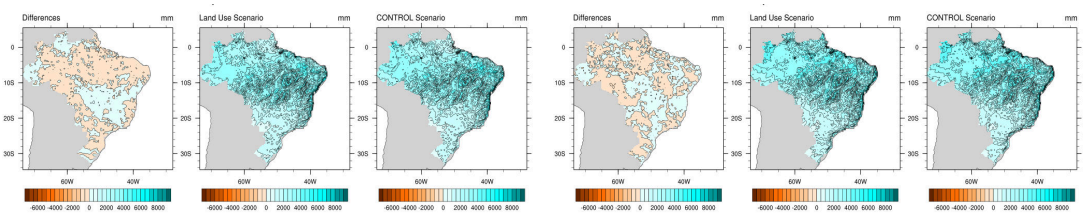

(a) 2001-2005

(b) 2005-2010

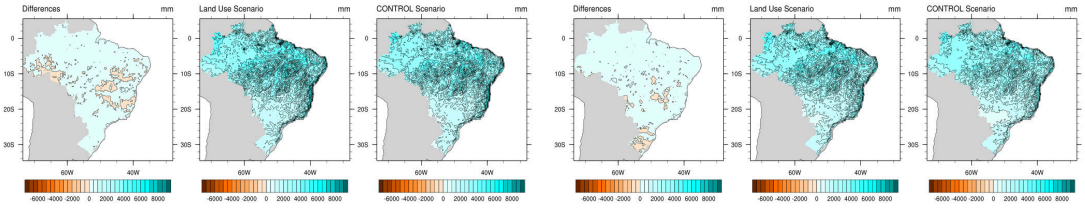

(c) 2011-2015

(d) 2016-2020

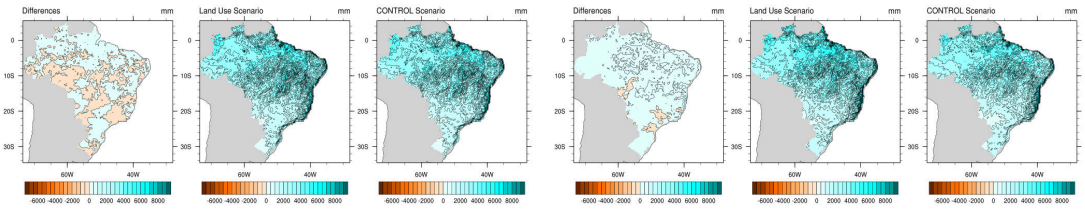

(e) 2021-2025

(f) 2026-2030

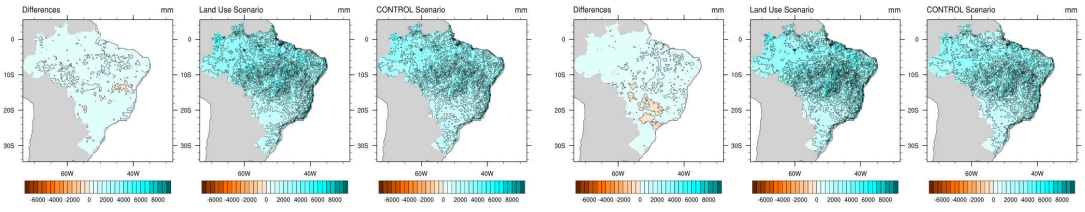

(g) 2031-2035

(h) 2036-2040

Figure 3.14: Contour plot of five-year average of the total precipitation [mm/day] in Brazil

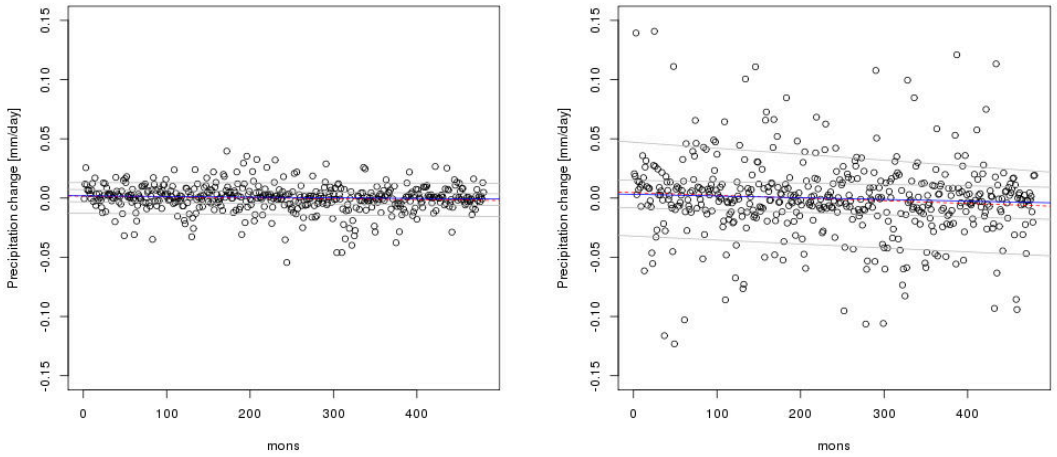

(a) Brazil (b) Land use region

Figure 3.15: Quantile regression of the total precipitation [mm/day] for Brazil and the region of land use change

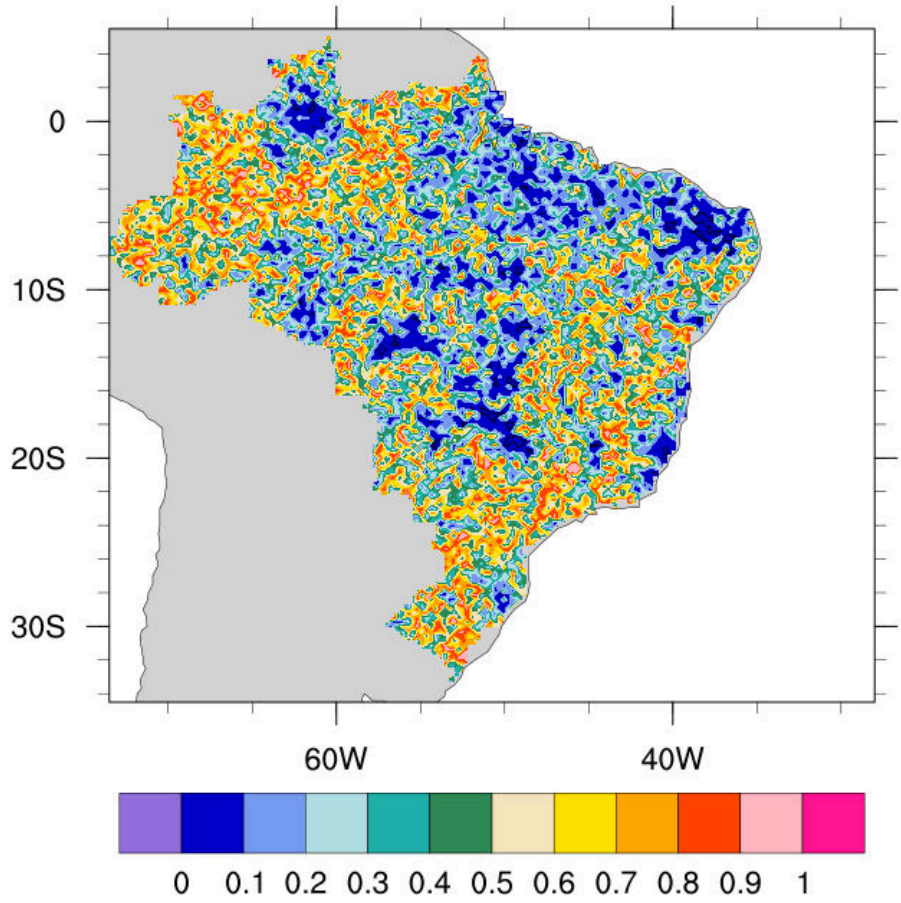

Figure 3.16: p values of the Chi-Square test. Lower values indicate higher significance of a change.

3.3 Evaporation

In the following chapter, the impact of the climate and the land use change on the evaporation is analyzed. First the climate impact is investigated. The difference in the five-year average between 2036–2040 and 2001–2005 is calculated for the CLT simulation: $\overline{E_{2036-2040}} - \overline{E_{2001-2005}}$. Over the larger parts of Brazil, the evaporation increases, with the strongest increase of up to 3.5 mm/day in the north of Brazil (the districts Amapá and Pará). In the south of Brazil (the district of Rio Grande do Sul), a decrease of the evaporation can be observed with up to -0.66 mm/day. Averaged over whole Brazil a slight increase of 0.10 mm/day.

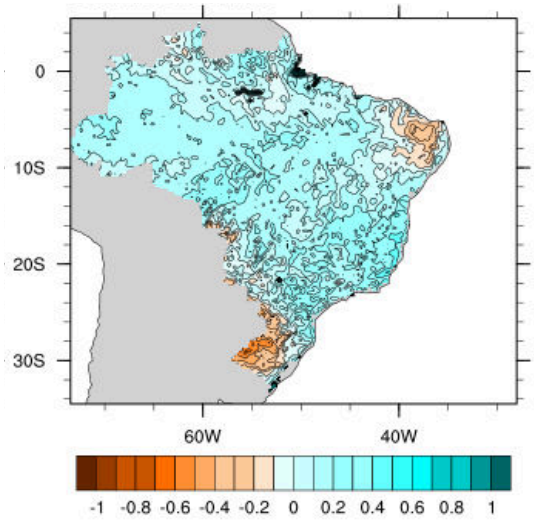

Figure 3.17: Climate change impact in the CTL simulations. Difference in the evaporation between 2036-2040 and 2001-2005.

The positive trend in the evaporation, can also be seen in the time series of the evaporation for both experiments $\{E_{CTL}\}$ and $\{E_{LUC}\}$ in Figure 3.18. The evaporation strongly varies over time due to the high variability in the ECHAM5 climate change forcing. Overall, the both experiments only differ slightly.

To further investigate the impact of the land use change on the evaporation on the entire period 2001–2040, the differences between both experiments are shown, for the total time period (Figure 3.19a), for the summer season (Figure 3.19b) and the winter season (Figure 3.19c). Neither for the entire time period nor for the two seasons a clear signal is evident. The evaporation changes slightly but in both directions (positive and negative). For central Brazil, the evaporation increases for the annual mean and for the winter season, but decreases for the summer season.

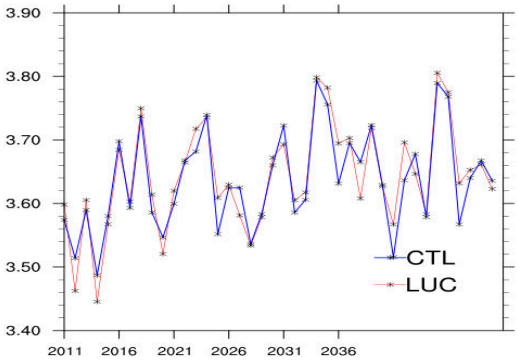

Figure 3.18: Time series of the Brazilian evaporation from 2001 to 2040 for the CTL simulations (blue) and the LUC simulations (red).

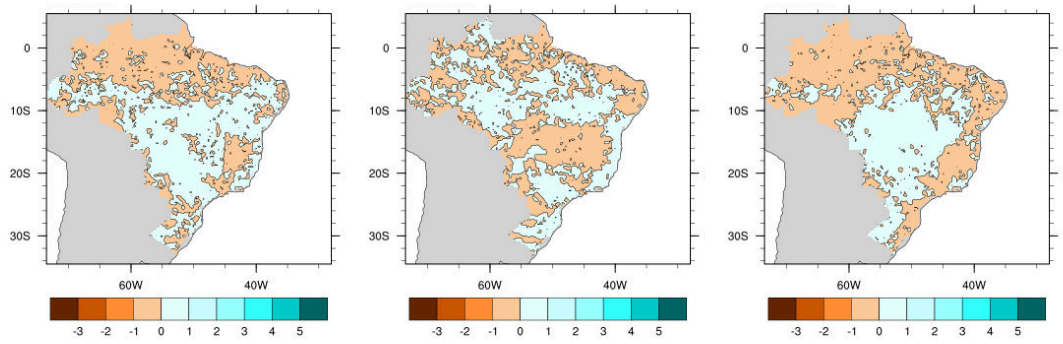

(a) 2001-2040 (b) DJF (c) JJA

Figure 3.19: Difference of the evaporation [mm/day] over the entire time series 2001–2040, summer and winter with respect to the reference period 2001–2005.

The strongest impact of the land use change can be seen in the annual cycle of the evaporation the region of the land use change (Figure 3.20b). The evaporation increases throughout the year due to land use change. This impact is based on the different evaporation rates of croplands and of savannas. Since these are local effects, no signal can be found takes place in the region of Brazil, the strongest increase in the evaporation takes place in summer. This fits to the expectations coming from the model set-up, where the surface moisture is increased by the land use change.

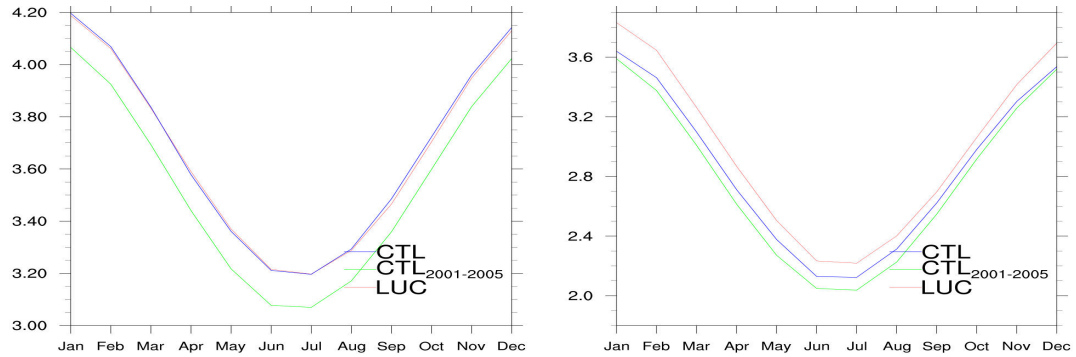

(a) Brazil (b) Land use region

Figure 3.20: Annual cycle of the evaporation [mm/day] for the period 2036-2040 for a) Brazil and b) LUC region.

Similar to the 2 m temperature and the total precipitation, the local effect of the land use change are investigated by calculating the average over the regions affected by the land use change. Similar results are obtained in regions with only a small land use change (e.g. Pará, Figure 3.21b) where no difference can be found. In Figure 3.21a, a positive trend in the difference between the LUC experiment and the CTL experiment, is evident. Districts in the south of Brazil have a higher variability in the evaporation compared to districts in the center and the north. The low variability near the equator can be explained by the fact that there the tropical rain forest is a constant source of evaporation.

The spatial change in evaporation for each five-year time slice is shown in Figure 3.22. In both experiments, a gradient with larger absolute values in the north of Brazil and with smaller values in the south of Brazil can be found (middle and right hand-side figures). In contrast to the spatial pattern in the precipitation change (see Figure 3.14) no constant change can be found in the evaporation. Changes in the evaporation are close to zero for all five-year time slices. Overall, I find an

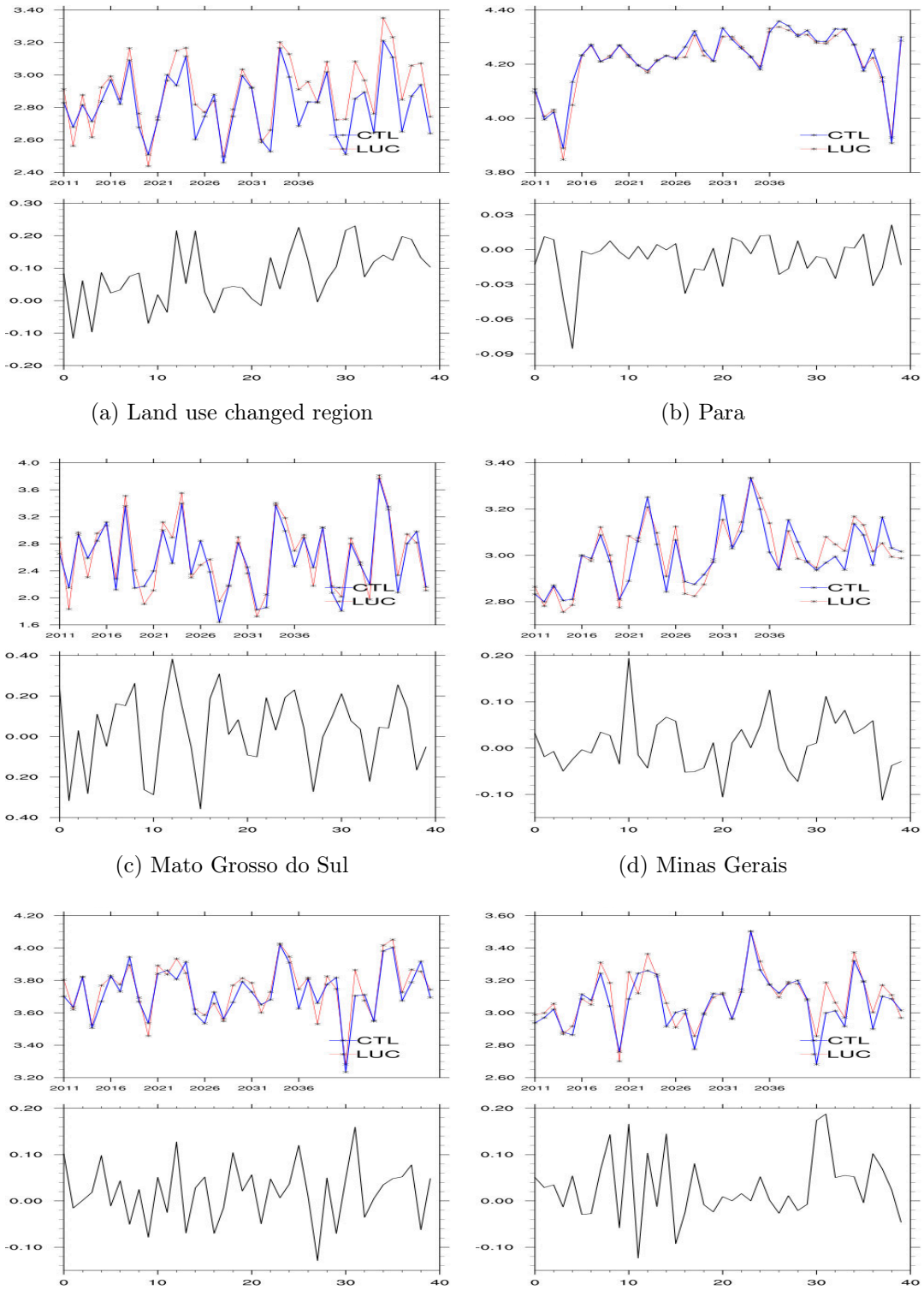

(a) Land use changed region

(b) Para

(c) Mato Grosso do Sul

(d) Minas Gerais

(e) Mato Grosso

(f) Goias

Figure 3.21: Area average of the time series of the evaporation [mm/day] over different regions.

increase in evaporation due to land use change, which is constrained to the area affected by land use change.

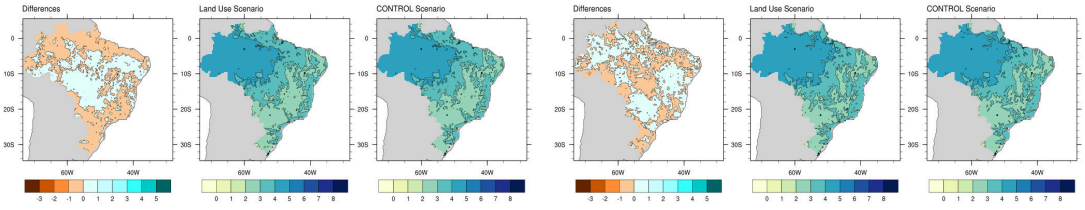

(a) 2001-2005

(b) 2005-2010

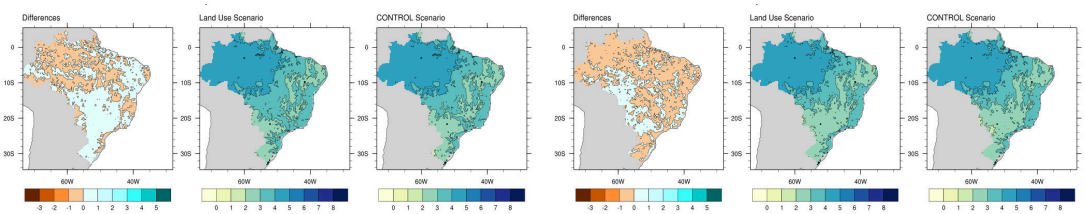

(c) 2011-2015

(d) 2016-2020

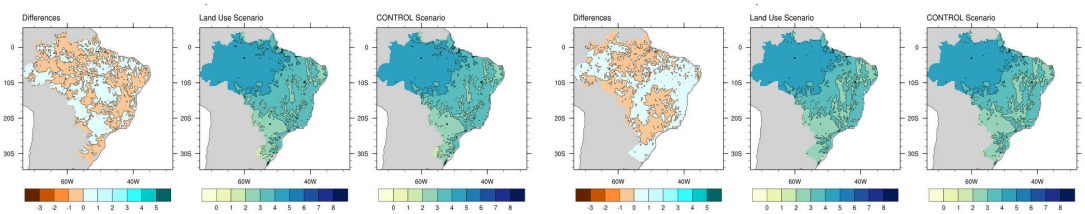

(e) 2021-2025

(f) 2026-2030

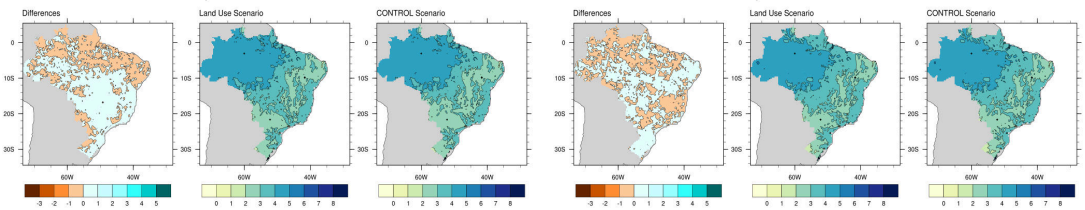

(g) 2031-2035

(h) 2036-2040

Figure 3.22: Contour plot of five-year average of the evaporation [mm/day] in Brazil.

3.4 Hydrological cycle

The water exchange between the surface and the atmosphere is investigated as the difference between precipitation and evaporation ($P - E$). This balance indicate the atmosphere gains or losses whether water to the soil. It can be directly linked to the latent heat flux, as discussed in Equation (1.3). Since the model excludes water sources or sinks in the soil, ($P - E$) is equivalent to the balance of the surface and the sub-surface runoff. ($P - E$) is the net water flux into the surface. Changes in the difference between precipitation and evaporation indicates a strengthening or weakening of the hydrological cycle.

The climate impact on the hydrological cycle is evaluated by the last five-year time slice (2036–2040) and the reference period (2001–2005) in the CTL experiment. (P-E) increases leading to a strengthening of the hydrological cycle in large parts of Brazil with the strongest positive signal in the district of Rio Grande do Sul (the southernmost district of Brazil). However, in some coastal areas, a decrease and therefore, a weakening of the hydrological cycle takes place.

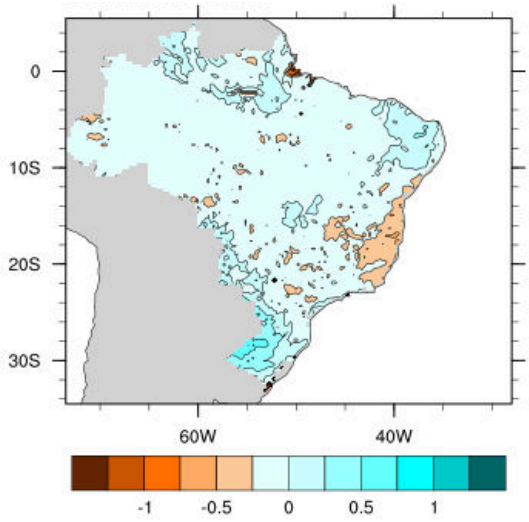

Figure 3.23: Climate change impact of P-E [mm/day] in the CTL simulations.

The impact of the land use change on each five-year time-slices is investigated in Figure 3.24. This variability is also evident in the time series of (P-E) averaged only over regions affected by land use change (see Figure 3.25). Similar as for the evaporation, lower variability is found for the equatorial regions. The temporal variability in (P-E) is large with some periods indicating a decrease over all Brazil (see Figure 3.24e), whereas other periods show an increase (see Figure 3.24g). Over

the regions of land use change (P-E) decreases with time leading to a weakening of the hydrological cycle due to land use change. This trend in the hydrological cycle is opposed to the trend due to increased greenhouse gases.

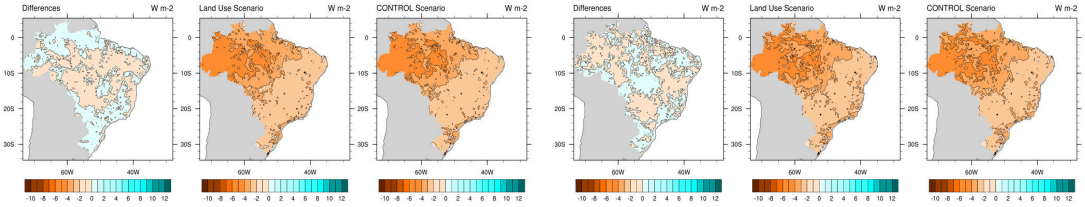

(a) 2001-2005

(b) 2005-2010

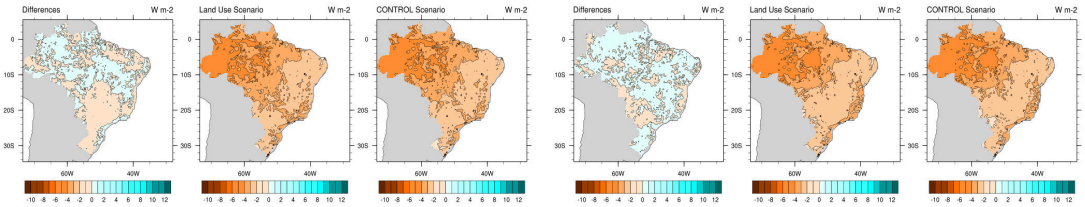

(c) 2011-2015

(d) 2016-2020

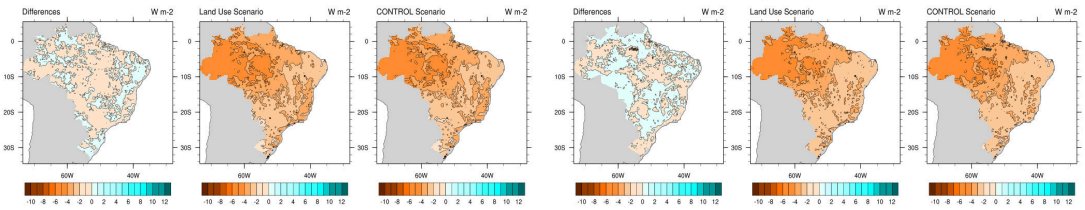

(e) 2021-2025

(f) 2026-2030

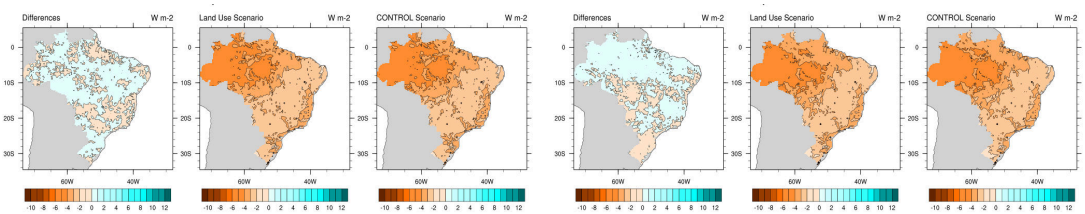

(g) 2031-2035

(h) 2036-2040

Figure 3.24: Contour plot of five-year average of the P-E [mm/day] in Brazil.

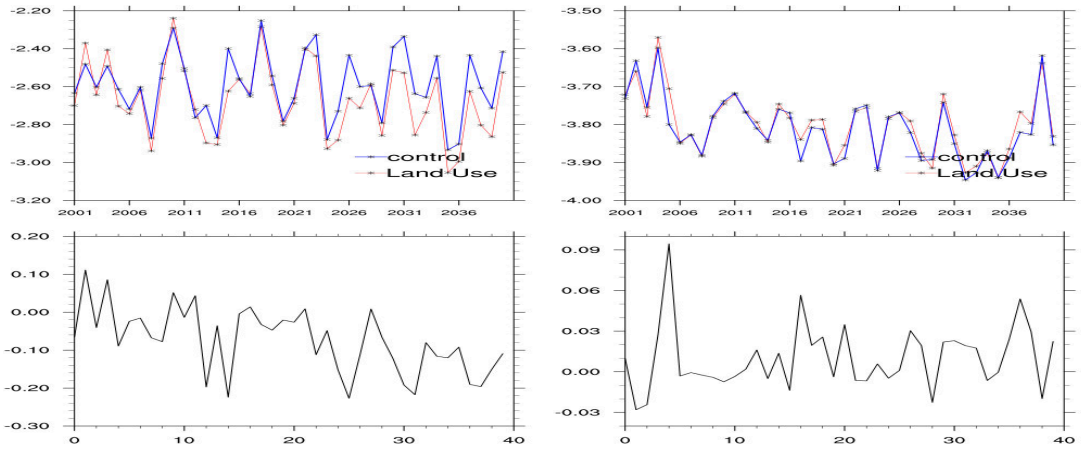

(a) Land use changed region

(b) Para

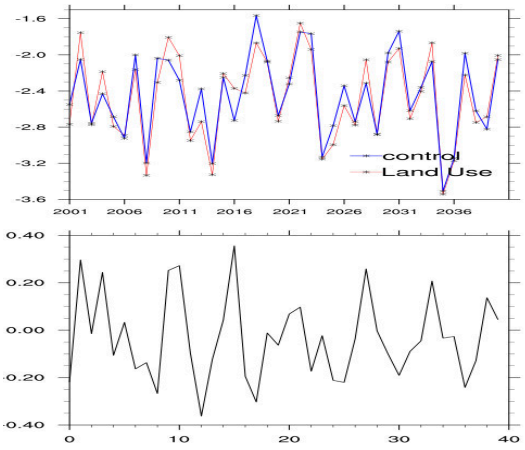

(c) Mato Grosso do Sul

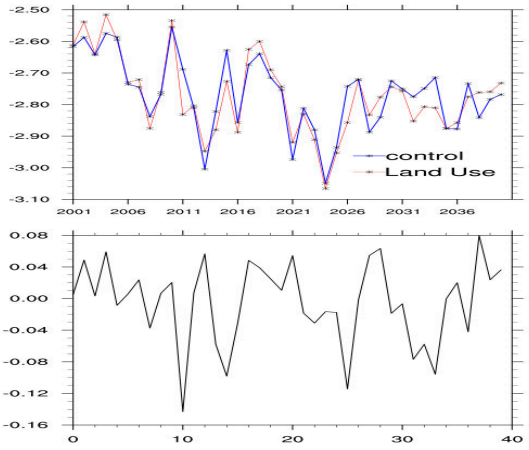

(d) Minas Gerais

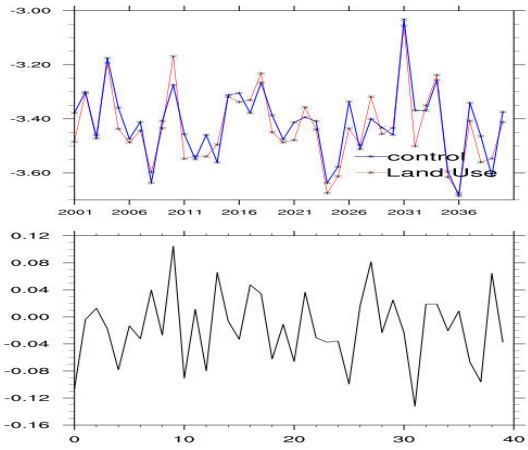

(e) Mato Grosso

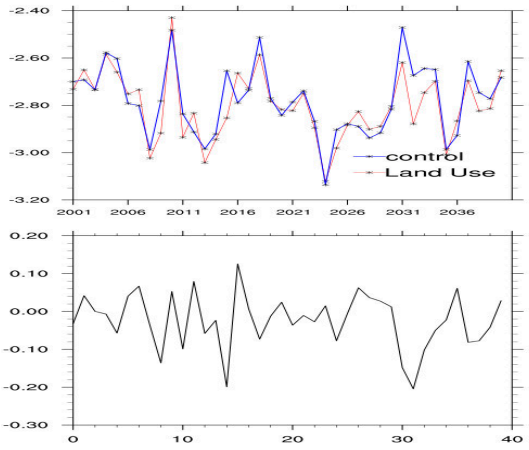

(f) Goias

Figure 3.25: Area average of the time series of P-E [mm/day] over different regions.

Chapter 4

Conclusion and Outlook

Before giving the final conclusion and an outlook, the results of the previous chapter are summarized.

The aim of this thesis is to investigate the climate variability and potential future climate change due to land use change in Brazil. A numerical down-scaling model is used to simulate the period from 2001 to 2040 in the region of South America. On a spatial grid of 60 km and 30 km the impact of land use and land cover changes are investigated. Two simulations are driven on the 30 km and 60km spatial grid. Where in the control simulation (CTL) the land use and land cover is fixed, the land use and land cover is updated every five years in the LUC experiment. Both experiments are driven by the ECHAM5 A1B greenhouse gas forcing. The main focus lies on the sensitivity of the hydrological cycle to land use change, studied by simulating the impact on the precipitation (P), evaporation (E), $P-E$ and the 2 m temperature. As a part of the CarBioCial project these results can be beneficial to the other project members to create a decision tool box for stakeholders and farmers in Brazil, to improve not only the environment but to also help the farmers to increase the crop production rates.

The results show that all variables increase until 2040 due to the impact of the greenhouse gas forcing. The strongest and clearest increase takes place in the 2 m temperature over whole Brazil. This temperature increase is in agreement with current studies (Christensen and Hewitson, 2007; Davidson and Metz, 2000; Marengo et al., 2010). The averaged precipitation over Brazil slightly decreases, however in most of the regions a precipitation increase occurs. An increase in the precipitation is in agreement with results presented by Li and Zeng (2002) and Vera et al. (2006). The evaporation as well as $(P-E)$ exhibit a positive trend due to the impact of the

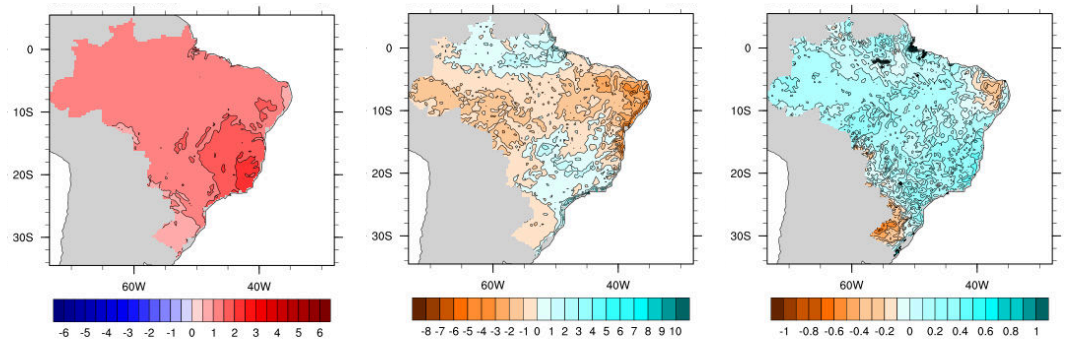

(a) 2 m temperature (b) total precipitation (c) evaporation

Figure 4.1: Impact of the climate change on the period 2036–2040 compared to the reference period 2001–2005 in the CTL experiment.

climate change. Figure 4.1 shows the results of the numerical and dynamical downscaling provided by the CTL experiment for the differences in five-year averaged time slice between 2036–2040 and the reference period 2001–2005.

Figure 4.2 illustrates the impact of the land use change on the temperature, precipitation and evaporation for the entire time period 2001–2040, in form of the differences between the LUC experiment and the CTL experiment, $\overline{X_{LUC}} - \overline{X_{CTL}}$.

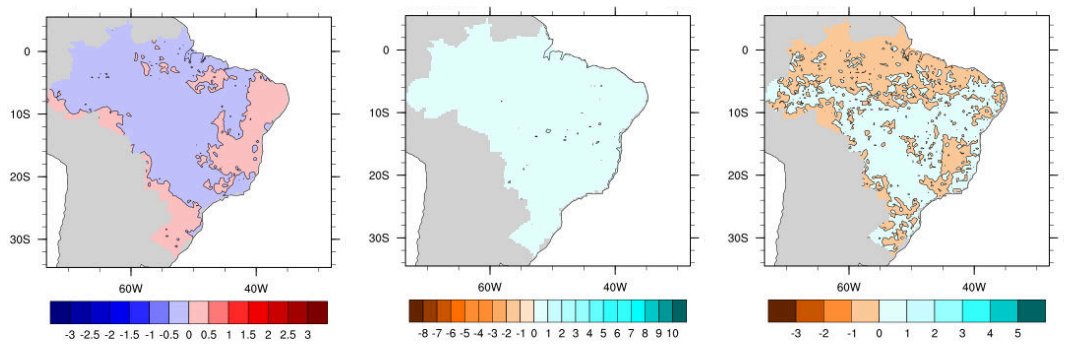

(a) 2 m temperature (b) total precipitation (c) evaporation

Figure 4.2: Impact of the climate change on the period 2001–2040 compared to the reference period 2001–2005 in the CTL experiment.

The effect of the land use change on most regions in Brazil is A cooling combined with an increase of precipitation. Since the land use change consists mostly of the conversion from savannas to cropland, the surface moisture increases and thus enhancing the evaporation. This evaporation increase is shown in Figure 4.2c. The cooling over the entire time period can be explained by an increase in evaporation,

which scales linearly with to the latent heat flux and evaporative cooling, and a decrease the albedo.

Due to the high variability in the analyzed variables the impact of the land use change is not necessarily seen in the time series. Furthermore, compared to the impact of the greenhouse gas forcing the impact of the land use change is small. This can be explained by the small area of the land use change compared with the entire domain. Small impacts are compared to the natural variability of the southern regions neglect able. These take place in mainly in two regions. The Pampas region in the south of Brazil where grassland are converted into croplands and the regions south of Amazonia where savanans are converted into croplands.

The effect of the land use change is found not only on a very local level, but also on a large scale (including whole Brazil), especially in the case of hydrological variables. These impacts correspond to findings of Shi et al. (2014). According to their study, the the impact of land use change as an effect of the changes in the hydrological cycle is dominating, the feedback mechanism, and not necessarily the change of the albedo.

Khanna et al. (2017) has shown that a change in the surface roughness can have a dominant effect. Lower surface roughness increases the near surface wind speed and supports evaporation and evapo-transpiration, which leads to a strengthening of the hydrological cycle.

In comparison with the effect of climate change (in this study represented by the ECHAM5 climate forcing) the effect of the land use change is counteracting, thus damping the climate change for the domain of Brazil. Nevertheless, huge, very important and fragile biomes can be destroyed.

My results indicate that the land use change can have an impact on the local and regional weather and climate system. However, to obtain more quantitative and robust information, additional future studies are needed. With this purpose I suggest to run ensemble simulations with and without a greenhouse gas forcing. Additionally, an ensemble simulation would help to examine the internal variability of the model and the variability induced by ENSO in the ECHAM5 simulations. State-of-the-art climate models contain a more realistic representation of the ENSO variability and should be used in a new set-up. They are based on representative concentration pathways (RCPs), which replaced the climate scenarios in previous GCM.

To identify the most suitable GCM for the region of Brazil, it would be helpful to use

a climate model selection toolbox, based on the performance of climate simulations in the past. The range of future climate scenarios could be evaluated by an envelope approach determine. Climate sensitivity studies could use this toolbox to investigate the impact of land use change on the full range of future climate simulations.

Local effects, e.g. the impact of the wind on the evaporation or the roughness length, could be investigated even more precise with a higher down-scaling up to few kilometers. Additionally, the extreme value theory could help to investigate local changes in extreme events. Especially in the last decades Brazil had to face extreme events. Climate sensitivity studies with implemented land use changes can help to evaluated the risk of future extreme events.

References

Arias, P. A., Fu, R., Hoyos, C. D., Li, W., and Zhou, L. (2011). Changes in cloudiness over the Amazon rainforests during the last two decades: diagnostic and potential causes. *Climate Dynamics*, 37(5-6):1151–1164.

Barros, V., Gonzalez, M., Liebmann, B., and Camilloni, I. (2000). Influence of the South Atlantic convergence zone and SouthAtlantic Sea surface temperature on interannual summerrainfall variability in Southeastern South America. *Theor. Appl. Climatol.*, 67(3):123–133.

Bush, M., Correa-Metrio, A., McMichael, C., Sully, S., Shadik, C., Valencia, B., Guilderson, T., Steinitz-Kannan, M., and Overpeck, J. (2016). A 6900-year history of landscape modification by humans in lowland Amazonia. *Quaternary Science Reviews*, 141:52–64.

Carvalho, L. M. V., Jones, C., Silva, A. E., Liebmann, B., and Silva Dias, P. L. (2011). The South American Monsoon System and the 1970s climate transition. *Int. J. Climatol.*, 31(8):1248–1256.

Charney, J., Stone, P. H., and Quirk, W. J. (1975). Drought in the sahara: a biogeophysical feedback mechanism. *Science*, 187(4175):434–435.

Chen, F. and Dudhia, J. (2001). Coupling an Advanced Land SurfaceâĂŞHydrology Model with the Penn StateâĂŞNCAR MM5 Modeling System. Part I: Model Implementation and Sensitivity. *Monthly Weather Review*, 129(4):569–585.

Christensen, J. and Hewitson, B. (2007). Regional Climate Projections. *Climate Change 2007: The Physical Science Basis*, 27(2007):847–940.

Costa, M. H. and Pires, G. F. (2010). Effects of Amazon and Central Brazil deforestation scenarios on the duration of the dry season in the arc of deforestation. *International Journal of Climatology*, 30(13):1970–1979.

Dai, A. (2006). Recent climatology, variability, and trends in global surface humidity. *Journal of Climate*, 19(15):3589–3606.

Dai, A. and Wigley, T. M. L. (2000). Global patterns of ENSO-induced precipitation. *Geophys. Res. Lett.*, 27(9):1283–1286.

Davidson, O. and Metz, B. (2000). Summary for Policymakers: Emissions Scenarios. A Special Report of Working Group III of the Intergovernmental Panel on Climate Change. *IPCC*, page 20.

Dee, D. P., Uppala, S. M., Simmons, A. J., Berrisford, P., Poli, P., Kobayashi, S., Andrae, U., Balmaseda, M. A., Balsamo, G., Bauer, P., Bechtold, P., Beljaars, A. C. M., van de Berg, L., Bidlot, J., Bormann, N., Delsol, C., Dragani, R., Fuentes, M., Geer, A. J., Haimberger, L., Healy, S. B., Hersbach, H., Hólm, E. V., Isaksen, L., Kållberg, P., Köhler, M., Matricardi, M., McNally, A. P., Monge-Sanz, B. M., Morcrette, J.-J., Park, B.-K., Peubey, C., de Rosnay, P., Tavolato, C., Thépaut, J.-N., and Vitart, F. (2011). The ERA-Interim reanalysis: configuration and performance of the data assimilation system. *Quart. J. Roy. Meteor. Soc.*, 137(656):553–597.

Dias, L. C., Pimenta, F. M., Santos, A. B., Costa, M. H., and Ladle, R. J. (2016). Patterns of land use, extensification, and intensification of Brazilian agriculture. pages 2887–2903.

Dudhia, J. (1989). Numerical Study of Convection Observed during the Winter Monsoon Experiment Using a Mesoscale Two-Dimensional Model.

ENREDD+ (2016). ENREDD+ National REDD+ Strategy. Technical report, Ministry of the Enviroment, Brazil.

Fersch, B. (2011). *Large scale water balance estimation from downscaled atmospheric moisture budgets and evaluation with global climatological data sets and the GRACE spaceborne gravimetry.* Dissertation, University of Augsburg.

Friedl, M. A., Mciver, D. K., Zhang, X. Y., Muchoney, D., Strahler, A. H., Woodcock, C. E., Gopal, S., Schneider, A., Cooper, A., Baccini, A., Gao, F., and Schaaf, C. (2002). Global land cover mapping from MODIS: algorithms and early results. 83:287–302.

Grimm, A. M. and Natori, A. A. (2006). Climate change and interannual variability of precipitation in South America. *Geophysical Research Letters*, 33(19):L19706.

Guimberteau, M., Ciais, P., Ducharne, A., Boisier, J. P., Dutra Aguiar, A. P., Biemans, H., De Deurwaerder, H., Galbraith, D., Kruijt, B., Langerwisch, F., Poveda, G., Rammig, A., Rodriguez, D. A., Tejada, G., Thonicke, K., Von Randow, C., Von Randow, R. C. S., Zhang, K., and Verbeeck, H. (2017). Impacts of future deforestation and climate change on the hydrology of the Amazon Basin: a multi-model analysis with a new set of land-cover change scenarios. *Hydrology and Earth System Sciences*, 21(3):1455–1475.

Hong, S. and Lim, J. (2006). The WRF single-moment 6-class microphysics scheme (WSM6).

Imbach, P., Manrow, M., Barona, E., Barretto, A., Hyman, G., and Ciais, P. (2015). Spatial and temporal contrasts in the distribution of crops and pastures across Amazonia: A new agricultural land use data set from census data since 1950. pages 898–916.

Jungclaus, J. H., Keenlyside, N., Botzet, M., Haak, H., Luo, J.-J., Latif, M., Marotzke, J., Mikolajewicz, U., and Roeckner, E. (2006). Ocean Circulation and Tropical Variability in the Coupled Model ECHAM5/MPI-OM. *Journal of Climate*, 19(16):3952–3972.

Kain, J. S. (2004). The KainâĂŞFritsch Convective Parameterization: An Update. *Journal of Applied Meteorology*, 43(1):170–181.

Khanna, J., Medvigy, D., Fueglistaler, S., and Walko, R. (2017). Regional dry-season climate changes due to three decades of Amazonian deforestation. *Nature Climate Change*, 7:200–206.

Kim, H. H. (1992). Urban heat island. *Int. J. Remote sensing*, 13:2319–2336.

Koch, J., Schaldach, R., and Köchy, M. (2008). Modeling the impacts of grazing land management on land-use change for the Jordan River region. *Global and Planetary Change*, 64(3-4):177–187.

Lapola, D. M., Priess, J. a., and Bondeau, A. (2009). Modeling the land requirements and potential productivity of sugarcane and jatropha in Brazil and India using the LPJmL dynamic global vegetation model. *Biomass and Bioenergy*, 33(8):1087–1095.

Lapola, D. M., Schaldach, R., Alcamo, J., Bondeau, A., Koch, J., Koelking, C., and Priess, J. a. (2010). Indirect land-use changes can overcome carbon savings from

biofuels in Brazil. *Proceedings of the National Academy of Sciences of the United States of America*, 107(8):3388–93.

Lawrence, D. and Vandecar, K. (2014). Effects of tropical deforestation on climate and agriculture. *Nature Climate Change*, 5(1):27–36.

Leite, C. C., Costa, M. H., Soares-Filho, B. S., and de Barros Viana Hissa, L. (2012). Historical land use change and associated carbon emissions in Brazil from 1940 to 1995. *Global Biogeochemical Cycles*, 26(2).

Lejeune, Q., Davin, E. L., Guillod, B. P., and Seneviratne, S. I. (2014). Influence of Amazonian deforestation on the future evolution of regional surface fluxes, circulation, surface temperature and precipitation. *Climate Dynamics*, 44(9-10):2769–2786.

Li, J. and Zeng, Q. (2002). A unified monsoon index. *Geophys. Res. Lett.*, 29(8):1274.

Liebmann, B., Kiladis, G. N., Marengo, J., Ambrizzi, T., and Glick, J. D. (1999). Submonthly Convective Variability over South America and the South Atlantic Convergence Zone. *J. Climate*, 12(7):1877–1891.

Liebmann, B. and Mechoso, C. R. (2011). The South American monsoon system. In Chang, C.-P., Ding, Y., and Lau, N.-C., editors, *The Global Monsoon System - Research and Forecast*, chapter 9. World Scientific, 2 edition.

Madden, R. A. and Julian, P. R. (1971). Detection of a 40-50 Day Oscillation in the Zonal Wind in the Tropical Pacific. *Journal of the Atmospheric Sciences*, 28(5):702–708.

Mahmood, R., Quintanar, A. I., Conner, G., Leeper, R., Dobler, S., Pielke, R. A., Beltran-Przekurat, A., Hubbard, K. G., Niyogi, D., Bonan, G., Lawrence, P., Chase, T., McNider, R., Wu, Y., McAlpine, C., Deo, R., Etter, A., Gameda, S., Qian, B., Carleton, A., Adegoke, J. O., Vezhapparambu, S., Asefi, S., Nair, U. S., Sertel, E., Legates, D. R., Hale, R., Frauenfeld, O. W., Watts, A., Shepherd, M., Mitra, C., Anantharaj, V. G., Fall, S., Chang, H.-I., Lund, R., Treviño, A., Blanken, P., Du, J., and Syktus, J. (2010). Impacts of Land Use/Land Cover Change on Climate and Future Research Priorities. *Bulletin of the American Meteorological Society*, 91(1):37–46.

Malhado, A. C. M., Pires, G. F., and Costa, M. H. (2010). Cerrado Conservation is Essential to Protect the Amazon Rainforest. *AMBIO*, 39(8):580–584.

Marengo, J. A., Ambrizzi, T., da Rocha, R. P., Alves, L. M., Cuadra, S. V., Valverde, M. C., Torres, R. R., Santos, D. C., and Ferraz, S. E. T. (2010). Future change of climate in South America in the late twenty-first century: intercomparison of scenarios from three regional climate models. *Climate Dynamics*, 35(6):1073–1097.

Marengo, J. A., Jones, R., Alves, L. M., and Valverde, M. C. (2009). Future change of temperature and precipitation extremes in South America as derived from the PRECIS regional climate modeling system. *International Journal of Climatology*, 29(15):2241–2255.

Marris, E. (2005). The forgotten ecosystem. *Nature*, 437(October):944–945.

Mlawer, E. J., Taubman, S. J., Brown, P. D., Iacono, M. J., and Clough, S. A. (1997). Radiative transfer for inhomogeneous atmospheres: RRTM, a validated correlated-k model for the longwave. *Journal of Geophysical Research*, 102(D14):16663.

Müller, W. A. and Roeckner, E. (2008). ENSO teleconnections in projections of future climate in ECHAM5/MPI-OM. *Climate Dynamics*, 31(5):533–549.

Nobre, C. A., Sampaio, G., Borma, L. S., Castilla-Rubio, J. C., Silva, J. S., and Cardoso, M. (2016). Land-use and climate change risks in the Amazon and the need of a novel sustainable development paradigm. *Proceedings of the National Academy of Sciences*, 113(39):10759–10768.

Oke, T. (1973). City Size and the Urban Heat Island. *Atmospheric Environment*, 7:769–779.

Peixoto, J. P. and Oort, A. H. (1984). Physics of climate. *Reviews of Modern Physics*, 56:365–429.

Pielke, R. A., Pitman, A., Niyogi, D., Mahmood, R., McAlpine, C., Hossain, F., Goldewijk, K. K., Nair, U., Betts, R., Fall, S., Reichstein, M., Kabat, P., and de Noblet, N. (2011). Land use/land cover changes and climate: Modeling analysis and observational evidence. *Wiley Interdisciplinary Reviews: Climate Change*, 2(6):828–850.

Pires, G. F. and Costa, M. H. (2013). Deforestation causes different subregional effects on the Amazon bioclimatic equilibrium. *Geophysical Research Letters*, 40(14):3618–3623.

Pongratz, J., Bounoua, L., DeFries, R. S., Morton, D. C., Anderson, L. O., Mauser, W., and Klink, C. A. (2006). The Impact of Land Cover Change on Surface Energy and Water Balance in Mato Grosso, Brazil. *Earth Interactions*, 10(19):1–17.

Rieck, M. (2015). *The Role of Heterogeneities and Land-Atmosphere Interactions in the Development of Moist Convection*. PhD thesis.

Rieck, M., Hohenegger, C., and van Heerwaarden, C. C. (2014). The Influence of Land Surface Heterogeneities on Cloud Size Development. *Monthly Weather Review*, 142(10):3830–3846.

Robertson, A. W. and Mechoso, C. R. (2000). Interannual and Interdecadal Variability of the South Atlantic Convergence Zone. *Mon. Wea. Rev.*, 128(8):2947–2957.

Roeckner, E., Bäuml, G., Bonaventura, L., Brokopft, R., Esch, M., Giorgetta, M., Hagemann, S., Kirchner, I., Kornblueh, L., Manzini, E., Rhodin, A., Schlese, U., Schulzweida, U., and Tompkins, A. (2003). The atmospheric general circulation model ECHAM5 -Part I : Model description. *MIP Report*, 349:127pp.

Ruiz, J. J., Saulo, C., and Nogués-Paegle, J. (2010). WRF Model Sensitivity to Choice of Parameterization over South America: Validation against Surface Variables. *Monthly Weather Review*, 138(8):3342–3355.

Salazar, Á. (2016). *Assessing the Impacts of Land Cover Change on Climate in non-Amazonian South America*. PhD thesis.

Schaldach, R. and Koch, J. (2009). Conceptual design and implementation of a model for the integrated simulation of large-scale land-use systems. In Athanasiadis, I. N., Rizzoli, A. E., Mitkas, P. A., and Gómez, J. M., editors, *Proceedings of the 4th International ICSC Symposium Thessaloniki, Greece, May 28-29, 2009*, pages 425–438. Springer Berlin Heidelberg, Berlin, Heidelberg.

Schaldach, R., Wimmer, F., Koch, J., Volland, J., Geißler, K., and Köchy, M. (2013). Model-based analysis of the environmental impacts of grazing manage-

ment on Eastern Mediterranean ecosystems in Jordan. *Journal of Environmental Management*, 127:S84–S95.

Shi, Q., Yan, H., Qu, R., and Li, Z. (2014). *Projected Impacts of Cultivated Land Changes on Surface Climates in China*, chapter 4, pages 95–133. Springer Berlin Heidelberg, Berlin, Heidelberg.

Skamarock, W. C., Klemp, J. B., Dudhia, J., Gill, D. O., Barker, D. M., Duda, M. G., Huang, X.-y., Wang, W., Powers, J. G., and Division, M. M. (2008). A Description of the Advanced Research WRF Version 3. Technical Report June.

Spangler, K. R., Lynch, A. H., and Spera, S. A. (2017). Precipitation Drivers of Cropping Frequency in the Brazilian Cerrado: Evidence and Implications for Decision-Making. *Weather, Climate, and Society*, 9(2):201–213.

Stocker, T., Qin, D., Plattner, G.-K., Tignor, M., Allen, S., Boschung, J., Nauels, A., Xia, Y., Bex, V., and Midgley, P. (2013). *Climate Change 2013: The Physical Science Basis. Contribution of Working Group I to the Fifth Assessment Report of the Intergovernmental Panel of Climate Change*. Cambridge University Press, New York.

Strahler, A., Muchoney, D., Borak, J., Friedl, M., Gopal, S., Lambin, E., and Moody, A. (1999). MODIS Land Cover Product Algorithm Theoretical Basis Document (ATBD) MODIS Land Cover and Land-Cover Change. (May):72.

Swann, A. L., Longo, M., Knox, R. G., Lee, E., and Moorcroft, P. R. (2015). Future deforestation in the Amazon and consequences for South American climate. *Agricultural and Forest Meteorology*, 214-215:12–24.

Trenberth, K. E. (1997). The Definition of El Niño. *Bulletin of the American Meteorological Society*, pages 2771–2777.

Trenberth, K. E., Smith, L., Qian, T., Dai, A., and Fasullo, J. (2006). Estimates of the Global Water Budget and Its Annual Cycle Using Observational and Model Data. *Journal of Hydrometeorology*, 8:758–769.

UNEP (2007). Global Environment Outlook. *Population and Development Review*, 4:572.

Vera, C., Silvestri, G., Liebmann, B., and González, P. (2006). Climate change scenarios for seasonal precipitation in South America from IPCC-AR4 models. *Geophysical Research Letters*, 33(13):L13707.

Warren, S. G., Eastman, R. M., and Hahn, C. J. (2007). A survey of changes in cloud cover and cloud types over land from surface observations, 1971-96. *Journal of Climate*, 20(4):717–738.

Zalasiewicz, J., Waters, C. N., Williams, M., Barnosky, A. D., Cearreta, A., Crutzen, P., Ellis, E., Ellis, M. A., Fairchild, I. J., Grinevald, J., Haff, P. K., Hajdas, I., Leinfelder, R., Mcneill, J., Richter, D., Steffen, W., Summerhayes, C., Odada, E. O., Syvitski, J. P. M., Vidas, D., Wagreich, M., Wing, S. L., Wolfe, A. P., Zhisheng, A., and Oreskes, N. (2015). Quaternary International. 383:196–203.

Zalasiewicz, J., Williams, M., Smith, A., Barry, T. L., Coe, A. L., Bown, P. R., Brenchley, P., Cantrill, D., Gale, A., Gibbard, P., Gregory, F. J., Hounslow, M. W., Kerr, A. C., Knox, R., Powell, J., Waters, C., Marshall, J., Oates, M., Rawson, P., and Stone, P. (2008). Are we now living in the Anthropocene? (2):4–8.

Zemp, D. C., Schleussner, C.-F., Barbosa, H. M. J., and Rammig, A. (2017). Deforestation effects on Amazon forest resilience. *Geophysical Research Letters*, 44(12):6182–6190.

List of Abbreviations

CAPE	convective available potential energy
CTL	control experiment
ECMWF	European Centre for Medium-Range Weather Forecasts
GCM	Global climate model
GEO4	Global Environment Outlook 4
ITCZ	Inner tropical convergence zone
KF	Kain-Fritsch scheme
LandSHIFT	Land Simulation to Harmonize and Integrate Freshwater Availability and the Terrestrial Environment
LUC	land use change experiment
LUCC	Land use / Land cover change
MJO	Madden-Julian Oscillation
MM5	Mesoscale Meteorology Model 5
NMM	Non-hydrostatic Mesoscale Model
NWP	Numerical weather prediction
RCM	Regional climate model
RRTM	Rapid Radiative Transit Model
SACZ	South American Convergence Zone
SAMS	South American Monsoon System
UNEP	United Nations Environment Programme
WRF	Weather Research and Forecasting model
WRF-ARW	Advance-Research WRF
WSM-6	WRF Single-Moment 6 Class Microphysics Scheme
YSU	Yonsei University scheme

Symbols

α	albedo
c_p	specific heat capacity of air
E	mass water evaporation rate
Δ	rate of change of saturation specific humidity with air temperature
G	ground heat flux
γ	psychrometric constant
g_a	conductivity of air
g_s	conductivity of stoma
H	sensible heat flux
λ	latent heat of vaporization
LH	latent heat flux
R_n	net surface energy
R_n	net radiation
ρ_a	dry air density

Appendix

```
&time_control
run_days      = 0,
run_hours     = 0,
run_minutes   = 0,
run_seconds   = 0,
start_year    = 2001, 2001, 2001, 2001, 2001, 2001,
start_month   = 01, 01, 01, 01, 01, 01,
start_day     = 01, 01, 01, 01, 01, 01,
start_hour    = 00, 00, 00, 00, 00, 00,
start_minute  = 00, 00, 00, 00, 00, 00,
start_second  = 00, 00, 00, 00, 00, 00,
end_year      = 2040, 2040, 2040, 2040, 2040, 2040,
end_month     = 12, 12, 12, 12, 12, 12,
end_day       = 31, 31, 31, 31, 31, 31,
end_hour      = 00, 00, 00, 00, 00, 00,
end_minute    = 00, 00, 00, 00, 00, 00,
end_second    = 00, 00, 00, 00, 00, 00,
interval_seconds = 21600
input_from_file = .true., .true.,
history_interval = 60, 60,
frames_per_outfile = 1, 1,
restart = .true.,
restart_interval = 2880,
io_form_history  = 2
io_form_restart  = 2
io_form_input    = 2
io_form_boundary = 2
io_form_auxinput4 = 2,
auxinput4_interval = 360, 360,
auxinput4_inname = "wrflowinp_d<domain>"
debug_level = 0,
io_form_auxinput2 = 2,
/
```

```
&dfi_control
 dfi_opt                             = 0
/

&domains
 time_step                           = 90,
 time_step_fract_num                 = 0,
 time_step_fract_den                 = 10,
 max_dom                             = 2,
 e_we                                = 106, 191,
 e_sn                                = 106, 191,
 e_vert                              = 45, 45,
 p_top_requested                     = 5000,
 num_metgrid_levels                  = 18,
 num_metgrid_soil_levels             = 4,
 dx                                  = 60000.0, 30000.0,
 dy                                  = 60000.0, 30000.0,
 grid_id                             = 1, 2,
 parent_id                           = 1, 1,
 i_parent_start                      = 1, 6,
 j_parent_start                      = 1, 6,
 parent_grid_ratio                   = 1, 2,
 parent_time_step_ratio              = 1, 2,
 feedback                            = 0,
 smooth_option                       = 2,
/

&physics
 mp_physics                          = 6, 6,
 ra_lw_physics                       = 1, 1,
 ra_sw_physics                       = 1, 1,
 radt                                = 15, 15,
 sf_sfclay_physics                   = 1, 1,
 sf_surface_physics                  = 2, 2,
 bl_pbl_physics                      = 1, 1,
 bldt                                = 0, 0,
```

```
 cu_physics                          = 1, 1,
 cudt                                = 5, 5,
 isfflx                              = 1,
 ifsnow                              = 0,
 icloud                              = 1,
 surface_input_source                = 1,
 num_soil_layers                     = 4,
 num_land_cat                        = 20,
 sf_urban_physics                    = 0,
 maxiens                             = 1,
 maxens                              = 3,
 maxens2                             = 3,
 maxens3                             = 16,
 ensdim                              = 144,
 sst_update                          = 0,
/

&dynamics
 w_damping = 1,
 diff_opt = 0,
 km_opt = 4,
 diff_6th_opt      = 0,
 diff_6th_factor = 0.12,
 base_temp = 290.,
 damp_opt = 3,
 zdamp = 5000., 5000.,
 dampcoef = 0.2,   0.2,
 khdif = 0, 0,
 kvdif = 0, 0,
 non_hydrostatic = .true., .true.,
 moist_adv_opt = 1, 1,
 scalar_adv_opt = 1, 1,
/

&bdy_control
 spec_bdy_width = 5,
```

```
 spec_zone = 1,
 relax_zone = 4,
 specified = .true., .true.,
 nested = .false., .false.,
/

&namelist_quilt
 nio_tasks_per_group = 0
 nio_groups = 1
/
```

List of Figures

List of Tables

Acknowledgments

First of all, I want to thank my supervisors Valerio Lucarini and Frank Lunkeit for the support and the many occasions where they gave me helpful advice during my PhD project. I am very thankful for the opportunity to write this thesis. I want to thank Frank Sielmann for all his technical expertise and his support to conduct the numerical simulations.

I like to express my gratitude to my colleagues in the group of Theoretical Meteorology, Christian Franzke, Richard Blender, Hartmut Borth, Silke Schubert, Tamas Bodai, Shabeh Ul Hasson and Valerio Lembo for having always an ear, for giving me advice and having an open ear for long discussions on my work.

Many thanks to Jürgen Böhner for his continued support of my thesis and my panel chair Herman Held.

I would also like to thank the SICSS graduate school for allowing me to have a fruitful exchange across different disciplines about my research project.

Thanks to the DKRZ for all their technical support and the tremendous amount of computational hours and disk space. All calculations and model experiments were carried out on the DKRZ (German Climate Computation Center) supercomputers blizzard, pitbull and mistral.

Let me also express my sincere thanks to the CarBioCial project which kicked off my thesis and the ClimateKIC project WINners which allowed my to continue my thesis. For this I want to thank Erik Chavez.

I am grateful to my fellow colleagues and friends for the incredible help, support, discussions, proofreading in the final days and just being there. Thanks so much to: Katharina Meraner, Jörg Burdanowitz, Nicole Burdanowitz, Sebastian Schubert, Gabriele Vissio, Maida Zahid and Melinda Galfi.

Ich möchte auch meiner Familie für die unendliche Unterstützung danken.

Eidesstattliche Versicherung
Declaration on Oath

Hiermit erkläre ich an Eides statt, dass ich die vorliegende Dissertationsschrift selbst verfasst und keine anderen als die angegebenen Quellen und Hilfsmittel benutzt habe.

I hereby declare, on oath, that I have written the present dissertation by myself and have not used other than the acknowledged resources and aids.

Hamburg, den 27. September 2017

Markus Kilian